A glycine zipper motif governs translocation of type VI secretion toxic effectors across the cytoplasmic membrane of target cells

Jemal Ali[1,2,3], Manda Yu[1#], Li-Kang Sung[1], Yee Wai Cheung[1], and Erh-Min Lai[1,2,4*]

[1] Institute of Plant and Microbial Biology, Academia Sinica, Taipei, Taiwan
[2] Molecular and Biological Agricultural Sciences Program, Taiwan International Graduate Program, National Chung-Hsing University and Academia Sinica, Taipei, Taiwan
[3] Graduate Institute of Biotechnology, National Chung-Hsing University, Taichung, Taiwan
[4] Biotechnology Center, National Chung-Hsing University, Taichung, Taiwan

Running title: Glycine zipper mediated effector entry

*Correspondence author

Institute of Plant and Microbial Biology, Academia Sinica

128, Sec. 2, Academia Road, Nankang, Taipei, Taiwan 11529

Tel: 886-2-27871158

E-mail: emlai@gate.sinica.edu.tw

#Current address

Department of Biological Sciences
University of Wisconsin-Milwaukee
Milwaukee, Wisconsin, USA

ABSTRACT

Type VI secretion systems (T6SSs) can deliver diverse toxic effectors into eukaryotic and bacterial cells. Although much is known about the regulation and assembly of T6SS, the translocation mechanism of effectors into the periplasm and/or cytoplasm of target cells remains elusive. Here we used the *Agrobacterium tumefaciens* DNase effector Tde1 to unravel the mechanism of translocation from attacker to prey. We demonstrate that Tde1 loading onto the secretion machinery is mediated via binding to its adaptor through the N-terminus, which harbours continuous copies of GxxxG motifs resembling the glycine zipper structure found in proteins involved in the membrane channel formation. By amino acid substitutions on a conserved glycine zipper motif, we showed $G^{39}xxxG^{43}$ motif governs the delivery into target cells by permeabilizing the cytoplasmic membrane. The findings demonstrate effector itself mediates target cell entry. Considering the widespread presence of GxxxG motifs in bacterial effectors and pore-forming toxins, we proposed that glycine zipper mediated permeabilization is a conserved mechanism used by bacterial effectors for translocation across target cell membranes.

Key words: Type VI secretion system, DNase effector, antibacterial, glycine zipper, translocation, *Agrobacterium tumefaciens*

INTRODUCTION

In a complex microbial community, bacteria have evolved versatile secretion systems for export or import of substrates across their membranes in response to different environmental cues. Each of specialized protein secretion systems (type I to X secretion system [TISS to TXSS]) [1,2,3] can recognize specific substrates for secretion and translocation across one or multiple membranes. The type VI secretion system (T6SS) is a molecular weapon deployed by many Proteobacteria for pathogenesis, antagonism, or nutrient acquisition [4]. The T6SS effectors discovered so far exert functions in antibacterial, anti-eukaryotic, and metal acquisition [5-8]. The most established T6SS effectors are

57 bacterial toxins, in which bacteria also produce cognate immunity proteins to prevent self-
58 intoxication and toxicity in the sibling cells.

59 T6SS is a multiprotein complex, composed of at least 13 conserved core proteins
60 resembling a phage tail structure, that extends from the cytoplasm to the outer membrane
61 of the attacker cell [9,10]. The T6SS machine consists of the Tss(J)LM membrane complex
62 (MC), Tss(A)EFGK base plate (BP), TssBC contractile sheath, and Hcp-VgrG-PAAR
63 puncturing device. The MC interacts with the BP [11,12], which serves as a docking site of
64 VgrG-PAAR effector complex to initiate polymerization of the tail [13]. The tail is composed
65 of the Hcp inner tube and TssBC outer sheath, and when triggered, the sheath contracts
66 and ejects out the effector decorated puncturing device into extracellular milieu or target
67 cells [14,15].

68 The T6SS has multiple strategies for delivering diverse effectors. On the basis of the
69 known effectors and their transport mechanisms, effectors can be classified as
70 "specialized" or "cargo" effectors [9,16]. Specialized effectors are fused to either of the C-
71 termini of three core structural proteins (Hcp, VgrG, or PAAR) while cargo effectors
72 interact directly or require a specific chaperone/adaptor to be loaded into the lumen of the
73 Hcp tube or onto the VgrG spike prior to secretion. Antibacterial effectors can act in the
74 cytoplasm, membrane, or periplasm of the target cells [5,6,8]. It is not known how effectors
75 that target the cytoplasm breach both the outer and inner membranes of target cells.

76 Glycine zipper structure consisting of repetitive GxxxG motifs is commonly found in
77 membrane-associated proteins [17] and bacterial toxins [18,19]. Glycine zipper motifs are
78 known be involved in toxicity of some bacterial effectors for membrane channel formation.
79 For examples, the transmembrane domain (TMD) of a vacuolating toxin, VacA of
80 *Helicobacter pylori* encodes three GxxxG motifs forming helix-helix packing interactions
81 [19], which are required for the vacuolation and membrane channelling contributing to VacA
82 toxicity [20]. Type I secretion effectors CdzC and CdzD of *Caulobacter crescentus* and
83 T6SS effector Tse4 of *Pseudomonas aeruginosa,* also possess glycine zipper motifs
84 involved in antibacterial activity [21,22]. Expression of Tse4 disrupted the proton motive force
85 of the inner membrane while CdzC and CdzD form surface aggregation for contact-

86 dependent killing of target cells. However, how glycine zipper motifs of Tse4 and CdzCD
87 involved in toxicity remain unknown.

88 A T6SS-encoding locus is highly conserved in the genome of plant pathogenic bacterium
89 *Agrobacterium tumefaciens* and the apparatus functions as an antibacterial weapon [23-26].
90 We previously revealed that *A. tumefaciens* strain C58 deploys two Type VI DNase
91 effectors (Tde1 and Tde2) as the major antibacterial weapons, in which the cognate
92 immunity proteins (namely Tdi1 and Tdi2) prevent autointoxication [23]. Both Tde1 and
93 Tde2 harbour a novel C-terminal Ntox15 toxin domain [27] containing an HxxD catalytic
94 motif required for its DNase activity [23]. Tde1 requires its cognate chaperone/adaptor Tap1
95 for loading onto VgrG1 for secretion [28].

96 By obtaining an uncoupling Tde1 variant that remains capable for binding to Tap1 for
97 export but deficient in membrane permeability, we revealed the secretion and
98 translocation mechanism of Tde1 from the attacker cell to the target cell. We showed that
99 the N-terminal region of Tde1 harbouring repetitive glycine zipper motifs is sufficient for
100 interacting with Tap1 for secretion. Once secreted, a conserved glycine zipper motif is
101 necessary for translocation across target cell membranes. The findings demonstrate a
102 new role of glycine zipper motif(s) in effector delivery into target cells.

103

104 **RESULTS**

105 **Tde1 can cause DNase-independent growth inhibition of prey cells**

106 Our previous study showed that overexpression of Tde1 in *Agrobacterium tumefaciens*
107 C58 caused growth inhibition, and the immunity protein Tdi1 only partially protected
108 against this cytotoxicity [23]. We hypothesized that Tde1 has domains apart from the DNase
109 domain that contribute to its toxicity. In addition to the C-terminal Ntox15 DNase domain
110 (amino acid 99-247) [23], Tde1 has a predicted transmembrane domain (TMD, 22-42)
111 (Fig.1A). Thus, three fragments of Tde1, that being the N-terminal, N-Tde1(1-97) and two
112 C-terminal regions, C1-Tde1(49-278), and C2-Tde1(98-278) were tested for toxicity. To
113 avoid confounding effects by the DNase activity, substitutions of catalytic residues
114 (H190A, D193A) were introduced in the C1-Tde1 and the full length wide-type Tde1 to

115 become C1-Tde1(M) and Tde1(M) respectively (Fig.1A). Ectopic expression in
116 *Escherichia coli* (DH10B) under an IPTG inducible promoter showed that N-Tde1 was
117 sufficient to inhibit growth (Fig.1B). Tde1(M), but not the C1-Tde1(M), is growth inhibitory.
118 Surprisingly, C2-Tde1(WT), which retains the wild type DNase catalytic residues, was not
119 sufficient to inhibit growth. Evidence suggests the N-terminal region of Tde1 is sufficient
120 to confer toxicity under conditions tested and that the C-terminal DNase domain requires
121 the N-terminus for it to cause toxicity.

122 To test Tdi1, the immunity protein for the DNase toxicity of Tde1 [23], can also neutralize
123 the N-Tde1 toxicity, the Tde1 variants were co-expressed with the Tdi1. The result
124 showed that Tdi1 could not rescue the growth inhibition caused by the N-Tde1 and
125 Tde1(M) (Fig 1C). This indicates that Tdi1 cannot neutralize the N-terminus-mediated
126 toxicity.

127 **A glycine zipper motif in N-terminus of Tde1 is required for toxicity and enhanced**
128 **membrane permeability**

129 To get an insight into the cause of growth inhibition by N-terminus of Tde1, we used N-
130 Tde1 region as a query to search against the NCBI non redundant (nr) database and
131 identified Tde1 homologues encoded in the T6SS gene clusters of
132 *Agrobacterium/Rhizobium* as well as tape measure proteins (TMP) encoded in genomes
133 of *Paraburkholderia/Burkholderia* (Fig 1D, Fig S1). We noticed the striking conservation
134 of continuous copies of GxxxG motifs (12-51), which resembles the glycine zipper motifs
135 overrepresented in membrane proteins and reported to be involved in the membrane
136 channel formation [17]. Thus, we hypothesized that these repetitive glycine zipper motifs are
137 necessary for membrane permeability and are the cause for N-Tde1 toxicity.

138 To test this, two highly conserved glycine residues at position 39 and 43 of a glycine
139 zipper motif were substituted with leucine (G39L and G43L), and the resulting N-Tde1
140 and Tde1(M) variants were named as N-Tde1^{GLGL}, Tde1(M)^{GLGL} respectively. The growth
141 analysis of *E. coli* DH10B cells showed that both N-Tde1^{GLGL} and Tde1(M)^{GLGL} lost the
142 ability to cause growth inhibition (Fig.2A). Similar results were also observed when they
143 were overexpressed in *A. tumefaciens* Δ*tde1* mutant (Fig. S2), indicating that the
144 $G^{39}xxxG^{43}$ glycine zipper motif of Tde1 is responsible for the observed toxicity.

145 Next, we tested whether N-Tde1 can increase *E. coli* inner membrane permeability. To
146 do so, we used the β-galactosidase activity assay to measure the entry of ortho
147 nitrophenyl galactopyranoside (ONPG) (301 Da) into the cytosol. ONPG normally
148 requires a functional permease LacY to enter into the cytosol but can enter if the inner
149 membrane is permeabilized/compromised [29,30]. The N-Tde1 and Tde1(M) as well as their
150 glycine zipper substitution variants were expressed in *E. coli* BW25113Δ*lacY* [31] carrying
151 β-galactosidase (pYTA-*lacZ*). The BW25113Δ*lacY*(pYTA-*lacZ*) complemented with *lacY*
152 was used as a positive control.

153 The results showed that cells expressing either N-Tde1 or Tde1(M) had similar β-
154 galactosidase activity as LacY expressing cells. In contrast, cells expressing N-Tde1^{GLGL}
155 and Tde1(M)^{GLGL} only exhibited background level activity as the negative controls (Fig
156 2B). These results indicate that the N-Tde1 and Tde1(M) are able to increase membrane
157 permeability depending on the $G^{39}xxxG^{43}$ motif. The data also suggest that the N-
158 terminus-mediated growth inhibition is caused by its ability to enhance inner membrane
159 permeability through glycine zipper motifs.

160 To further analyse the extent of enhanced membrane permeabilization, cells from the
161 same experiment were normalized to the same OD_{600} and stained with Hoechst and
162 propidium iodide (PI). Hoechst (616 Da) is a nucleic acid staining dye which is permeable
163 to live Gram-negative bacterial cells while PI (668.4 Da) can enter through a compromised
164 inner membrane or dead cells. The PI/Hoechst staining showed strong PI signals in cells
165 expressing N-Tde1 and Tde1 (M) but no or weak signals were detected in cells expressing
166 N-Tde1^{GLGL}, Tde1(M)^{GLGL}, or vector control, indicating that N-Tde1 is able to enhance
167 membrane permeability to allow molecules with size 668.4 Da to pass (Fig 2C). Hoechst
168 signals were detected in all cells but stronger in cells expressing N-Tde1 or Tde1(M).

169 The cells used for membrane permeability assays were also collected for counting viable
170 cells. Accordingly, there was no obvious difference on the number of viable cells among
171 the strains tested (Fig 2D), suggesting that the detected enhanced PI fluorescence in cells
172 expressing N-Tde1 and Tde1(M) is due to compromised membrane permeabilization but
173 not cell death.

174 We next determined whether the N-terminus of Tde1 is bacteriostatic or bacteriolytic. *E.*
175 *coli* cells were induced with IPTG to express N-Tde1 or Tde1(M) and after one hr, washed
176 with fresh media without IPTG for continuous cultivation. We found that growth was
177 recovered when cells were washed of the IPTG inducer, in contrast to the growth inhibition
178 of cells with continuous IPTG induction (Fig 2E). The combined data suggest that the N-
179 terminus of Tde1 is sufficient to facilitate membrane permeability for bacteriostatic toxicity,
180 and such activity requires the conserved $G^{39}xxxG^{43}$ glycine zipper motif.

181 **The N-terminus of Tde1 is necessary and sufficient for Tap1 interaction**

182 Tap1 is the adaptor for loading Tde1 onto VgrG1 [23,28]. However, the mechanism that Tde1
183 and Tap1 interact remains undefined. We first performed co-immunoprecipitation (co-IP)
184 assay to identify the specific region of Tde1 that can interact with Tap1 in *A. tumefaciens*.
185 The HA-tagged Tde1 variants were expressed in Δ*tde1* and anti-HA agarose bead was
186 used to co-precipitate the interacting proteins followed by western blotting to detect Tde1
187 variants and Tap1. The results showed that the N-Tde1 and Tde1(M) interact with Tap1
188 but not the C-terminal variants, C1-Tde1(M) and C2-Tde1 (Fig.3A). N-Tde1^{GLGL} and
189 Tde1(M)^{GLGL} remain capable of interacting with Tap1 (Fig.3A).

190 Next, we determined whether the Tap1 can interact with Tde1 in *E. coli* where T6SS is
191 absent. Similar to the results in *A. tumefaciens,* the N-Tde1 and Tde1(M) interacted with
192 Tap1 but not the C-terminal variants (Fig. 3B). Tap1 interaction with N-Tde1^{GLGL} was also
193 detected, but since Tde1(M)^{GLGL} was unstable in *E. coli*, intact Tde1^{GLGL} was barely
194 detected and the interaction with Tap1 was similarly diminished (Fig. 3B). The co-IP
195 results in *A. tumefaciens* and *E. coli* together suggest that Tap1 interacts with Tde1
196 through the N-terminus and that the G39L and G43L substitution does not affect Tde1-
197 Tap1 interaction. However, $G^{39}xxxG^{43}$ motif is crucial to maintain integrity of Tde1(M)
198 when expressed in *E. coli* (Fig. 3B).

199 **The N-terminus of Tde1 is necessary and sufficient for secretion**

200 Because N-Tde1 interacts with Tap1, we hypothesized that this region is required for Tde1
201 secretion. Thus, we performed secretion assay by expressing the various HA-tagged
202 Tde1 variants in Δ*tdei,* a deletion mutant lacking both *tde1-tdi1* and *tde2-tdi2* toxin

203 immunity pairs. Both cellular and extracellular fractions were collected to determine their
204 expression and secretion, respectively. The results showed that indeed all Tde1 variants
205 containing N-terminus is secreted but not the C-terminus, C1-Tde1(M). The secretion was
206 in a T6SS-dependent manner as secretion was abrogated in Δ*tdei*Δ*tssK,* which lacks both
207 *tdei* and *tssk* encoding the baseplate component. N-Tde1^{GLGL} and Tde1(M)^{GLGL} are also
208 stably expressed and secreted (Fig. 3C). The data suggest that N-terminus of Tde1 is
209 necessary and sufficient for secretion and that the G39L and G43L substitution did not
210 interfere with the secretion capacity of Tde1. Accordingly, Hcp secretion levels are highly
211 correlated with Tap1-Tde1 interaction and secretion of Tde1 variants (Fig. 3C). The data
212 also confirmed the requirement of the Tap1-Tde1 interaction for Tde1 secretion and
213 supported our previous finding that Tde loading onto VgrG is critical for active T6SS
214 secretion [32].

215 **G^{39}xxxG^{43} motif of Tde1 is required for target cell delivery**

216 Because the G^{39}xxxG^{43} glycine zipper motif located in N-Tde1 increased the membrane
217 permeability but was not required for secretion, we hypothesized that G^{39}xxxG^{43} is
218 responsible for inserting Tde1 into the inner membrane and delivering it into the
219 cytoplasm of target cells. Here, we engineered each of Tde1 variants fused to super-
220 folder green fluorescence protein (sfGFP) with a flexible (GGGS) linker between Tde1
221 and sfGFP to avoid the Tde1 functional/structural interference by GFP. The sfGFP fused
222 Tde1 variants were expressed in *A. tumefaciens* Δ*tdei* and Δ*tdei*Δ*tssK* mutants. The
223 secretion assay results showed that N-Tde1-sfGFP and Tde1(M)-sfGFP but not C1-
224 Tde1(M)-sfGFP are secreted and the G39L and G43L substitution did not compromise
225 the secretion (Fig 4A). No proteins were observed in the extracellular fractions of
226 Δ*tdei1*Δ*tssk* mutants, demonstrating that T6SS-dependent secretion.

227 To investigate the translocation of Tde1 variants, we mixed *A. tumefaciens* Δ*tdei,*
228 expressing sfGFP-fused Tde1 variants, with *E. coli* cells expressing mCherry. *A.*
229 *tumefaciens* expressing sfGFP only (Vector-sfGFP) was used as a negative control. After
230 co-culture, we imaged populations for mCherry (false coloured in blue) and GFP (green)
231 to detect *E. coli* and *A. tumefaciens*, respectively. We merged images to identify cyan
232 colored cells (overlayed blue and green signals), which represent *E. coli* cells with

233 translocated Tde1 variants carrying sfGFP. We were able to observe cyan fluorescence
234 when *A. tumefaciens* expressing N-Tde1-sfGFP and Tde1(M)-sfGFP was co-cultured
235 with *E. coli* mCherry whereas the GFP and mCherry signals were not overlapped in the
236 *E. coli* cells co-cultured with *A. tumefaciens* strains expressing GFP only or sfGFP-fused
237 C1-Tde1(M), N-Tde1^{GLGL}, Tde1(M)^{GLGL} respectively (Fig. 4B). No cyan fluorescence was
238 observed when N-Tde1-sfGFP and Tde1(M)-sfGFP were expressed in the Δ*tdei1*Δ*tssk*
239 mutant as the attacker (Fig. S3).

240 The data suggested that Tde1 is translocated into target cells in a T6SS- and G^{39}xxxG^{43}-
241 dependent manner. Because N-Tde1^{GLGL}-sfGFP and Tde1(M)^{GLGL}-sfGFP could be
242 secreted but not translocated into target cells, G^{39}xxxG^{43} motif is necessary for delivering
243 Tde1 into the target cell.

244 **G^{39}xxxG^{43} is required for interbacterial competition but dispensable for DNase**
245 **activity**

246 To assess the role of the G^{39}xxxG^{43} motif for target cell intoxication in the context of cell-
247 cell contact, we further performed interbacterial competition assays. *A. tumefaciens* C58
248 Δ*tdei* expressing either Tde1-Tdi1 or its glycine zipper variant, Tde1^{GLGL}-Tdi1, was
249 competed with target *E. coli* (DH10B) cells. *A. tumefaciens* Δ*tdei* (Tde1-Tdei1*)* exhibited
250 a strong killing activity (~10^3-fold reduction of target cell survival) as compared to the
251 negative controls, the secretion deficient mutants Δ*tssL* and Δ*tdei*Δ*tssK* (Tde1-Tdei1*)* (Fig
252 5A). In contrast, no killing activity could be observed for *A. tumefaciens* Δ*tdei* expressing
253 Tde1(M)-Tdi1. The killing activity of Δ*tdei*(Tde1^{GLGL}-Tdi1*)* was largely compromised,
254 similar to that of negative controls. We also performed interbacterial competition assays
255 using *A. tumefaciens* strain 1D1609, which is susceptible to T6SS killing by C58 [33]. The
256 intra-species killing activity was weaker (~10^2-fold reduced target cell survival), but the
257 killing activity of Δ*tdei* (Tde1^{GLGL}-Tdi1*)* against 1D1609 was not detectable (Fig 5B). The
258 results together indicated that G^{39}xxxG^{43} motif is required for interbacterial competition at
259 both inter- or intra-species levels. We also performed a secretion assay of these *A.*
260 *tumefaciens* attacker strains and as expected, Tde1^{GLGL} proteins were secreted (Fig. 5C).
261 It is notable that Tde1^{GLGL} proteins accumulate at slightly lower levels to that of Tde1 and
262 Tde1(M), which also led to reduced secretion levels of Tde1^{GLGL} and Hcp.

263 Although the reduced secretion level may partly contribute to compromised killing effect
264 of Δ*tdei*(Tde1^{GLGL}-Tdi1*)*, the most plausible explanation is that Tde1^{GLGL} is unable to
265 mediate its translocation across target cell membranes. To exclude the possibility that
266 G39L and G43L substitution may influence its DNase activity, we perform *in vivo* plasmid
267 DNA degradation assay. Tde1, Tde1^{GLGL}, and Tde1(M) were each expressed by tightly
268 controlled arabinose-inducible promoter for *in vivo* plasmid DNA degradation assay in *E.*
269 *coli* BW25113 as described [23]. As expected, plasmid DNA was completely degraded in
270 cells expressing Tde1, but not in the negative controls, the cells without arabinose
271 induction or cells expressing Tde1(M). As for Tde1^{GLGL}, plasmid DNA was also degraded
272 but not as complete as Tde1 (Fig. 5D). This is not surprising because Tde1(M)^{GLGL} is
273 prone for degradation in *E. coli* (Fig. 3B). Indeed, no intact Tde1^{GLGL} could be detected,
274 in contrast to the abundance of Tde1 and Tde1(M) (Fig. 5D). We also generated single
275 G39L and G43L substitution variants (Tde1^{G39L} and Tde1^{G43L}) and found that both
276 Tde1^{G39L} and Tde1^{G43L} are stably expressed and exhibit wild-type level DNase activity.
277 The degree of plasmd DNA degration is also correlated with the growth inhibition effect
278 (Fig. 5E and Fig. S2C). The slightly recovery of Tde1^{GLGL} in growth inhibition is consistent
279 with the instability of Tde1^{GLGL}. The evidence that G39L and G43L substitution of Tde1
280 abolished inner membrane permeability, translocation, and interbacterial competition but
281 did not affect DNase activity and secretion of Tde1 suggested the G^{39}xxxG^{43} motif is
282 necessary for delivering Tde1 across the inner membrane into the cytoplasm of target
283 cells.

284

285 **DISCUSSION**

286 Through the dissection of Tde1 DNase effector, we provide strong evidence for a role of
287 the N-terminal glycine-zipper motif(s) of Tde1 in delivering the T6SS effector into target
288 cells. Here, we proposed a model explaining the loading, firing, and translocation of Tde1
289 (Fig 6). In *A. tumefaciens,* Tde1 DNase activity is neutralized by Tdi1 by binding to C-
290 terminal DNase domain while its N-terminal domain interacts with Tap1 for loading onto
291 VgrG1 (Step 1). The VgrG1-Tap1-Tde1-Tdi1 complex is then recruited onto membrane-
292 associated baseplate, which serves as a docking site for polymerization of Hcp tube and

293 TssBC sheath (Step 2). Upon TssBC sheath contraction (Step 3), Tap1 and Tdi1 may fall
294 off and Hcp-VgrG-Tde1 puncturing device is then ejected for secretion. In contact with a
295 target cell, Tde1 may be delivered to periplasm of the target cell where Tde1
296 permeabilises the inner membrane in a $G^{39}xxxG^{43}$ motif-dependent manner (Step 5).
297 Once delivered, Tde1 exerts its toxicity by attacking DNA for degradation (Step 6).

298 T6SS cargo effectors often require the specific chaperone/adaptor for loading onto
299 puncturing device for secretion. Our previous findings demonstrated that Tap1, a
300 DUF4123-containing protein, specifically interacts with Tde1 for loading onto VgrG1 for
301 secretion [23,28]. We now showed that N-terminal region of Tde1 is necessary and sufficient
302 for interaction with Tap1 for secretion and delivery into target cells. The evidence that
303 $Tde1^{GLGL}$ variant remains capable for binding to Tap1 for export but deficient in membrane
304 permeability and translocation demonstrated a distinct role of this $G^{39}xxxG^{43}$ motif in
305 target cell delivery. Among the nine classes of the Ntox15-containing proteins, the
306 majority of them including Tde1 belong to class I without detectable N-terminal domains
307 (Fig. S1). We identified the presence of glycine zipper motifs overlapping with
308 transmembrane domain (TMD) not only in N-terminal region of all Tde1 orthologs
309 encoded in Rhizobiaceae but also in C-terminal region of tape measure proteins (TMP)
310 encoded in genomes of *Paraburkholderia/Burkholderia,* likely as a prophage. TMP is a
311 phage protein suggested to have a channel forming activity [34,35] and as a determinant in
312 connecting host inner membrane proteins for injecting phage genome into bacterial host
313 cells [36]. Such conservation in Tde1 orthologs suggested that this glycine zipper-mediated
314 delivery could be a common strategy deployed by these bacterial effectors for
315 translocation across target cell membranes. To this end, whether other more distantly
316 related Ntox15-containing proteins or more broadly bacterial toxins harbouring C-terminal
317 toxin domain may also use N-terminal glycine zipper to mediate effector translocation
318 await future investigations. It would be also interesting to investigate whether TMP also
319 employs its C-terminal glycine zipper to mediate phage genome entry into host cells.

320 Previous study in *P. aeruginosa* showed that VgrG-loaded Tse6-EgaT6 complex is
321 sufficient to translocate across a lipid bilayer *in vitro* [37], suggesting a role of VgrG-effector
322 complex itself in inserting across the inner membrane of target cells. A recent study further

323 uncovered a widespread prePAAR motif in N-terminal TMDs of T6SS effectors involved
324 in interaction with Eag family chaperone for export [38]. The findings from the Tap1 and Eag
325 chaperone-mediated T6SS toxins led us to propose that the bacterial toxins harbouring a
326 N-terminal TMD may be protected by its cognate chaperone/adaptor from insertion into
327 membranes in the attacker cell. However, once the effector is secreted in the periplasm
328 of the target cell, specific motifs (such as glycine zippers or perhaps prePAAR) may
329 mediate TMD to insert into the inner membrane for the delivery into the cytoplasm.

330 A few membrane permeabilizing T6SS toxins have been reported. The *Vibrio cholerae*
331 VasX caused dissipation of membrane potential, leading to membrane permeabilization
332 of target bacterial cells similar to the Tme effectors of *V. parahaemolyticus,* which
333 represents a widespread family of T6SS effectors harbouring C-terminal TMD for
334 membrane disruption [39,40]. On the other hand, Tse4 disrupts the membrane potential and
335 forms a cation selective pore without membrane permeabilization where the pore cannot
336 even allow the permeability of a relatively smaller molecular weight (ONPG, 300 Da) [21].
337 Distinct from these toxins in which they confer pore forming activity for toxicity, the role of
338 glycine zipper(s) of Tde1 appears to enhance membrane permeability for bringing the
339 toxin domain into target cell cytoplasm.

340 To date, no structural information is available for Ntox15 superfamily proteins where Tde1
341 belongs. While N-terminus of Tde1 lacks sequence similarity to any of those known pore-
342 forming toxins, structural modelling showed structural similarity of two helixes containing
343 consecutive glycine zipper motifs to the pore forming domain of pyocin S5 [41] (Fig S4).
344 Pyocin S5 can cause ATP leakage and PI permeability [42] potentially to inner membrane
345 after translocation through FptA and TonB1 [41]. Tde1 allows the passage of relatively
346 larger molecule, PI (668 Da), suggesting that its N-terminal glycine zipper(s) may form
347 larger pores similar to pyocin S5. $G^{39}xxxG^{43}$ motif plays no role in DNase activity of Tde1
348 but is crucial for its protein stability. Tde1 with substitution of one of the two glycine
349 residues to leucine retains stability of intact proteins but Tde1 is prone for truncations and
350 degradation when both glycine residues are substituted to leucine. The instability is most
351 evident when ectopically expressed in *E. coli* and when retaining DNase activity. Single
352 glycine substitution ($Tde1^{G39L}$ and $Tde1^{G43L}$ variants) does not influence protein stability

353 may suggest that the adjacent glycine residues (G^{35} or G^{47}) are sufficient to compensate
354 the loss of one glycine of $G^{39}xxxG^{43}$ motif for structural integrity in both variants. The
355 importance of $G^{39}xxxG^{43}$ motif in Tde1 protein stability is consistent with the role of glycine
356 zippers in structural impact [17].

357 With the knowledge of effector translocation mechanisms, the bacterial protein secretion
358 apparatus also offers a strategy for use of effector translocation domain for delivering
359 heterologous proteins to specific cells. T6SS is a promising vehicle for such purpose
360 because effectors or secreted proteins appear to be delivered with their folded form,
361 unlike those to be transported as unfolded forms in most of other specialized secretion
362 systems [1]. Engineering T6SS carriers such as VgrG spikes to carry exogenous effectors
363 proteins into target cells are feasible but challenging [43-45]. By using a truncated variant of
364 PAAR, a recent study showed delivering exogenous T6SS effectors and Cre recombinase
365 for genetic modification in the target cells [46]. Our success in using N-Tde1 in the delivery
366 of sfGFP proteins into target *E. coli* cells where they exert fluorescence also suggested
367 potential applications of N-Tde1 for the delivery of proteins of interests such as genetic
368 modifiers. This strategy provides advantages over transforming foreign DNA for
369 expressing a protein of interest from creating undesired genome manipulation.

370

371 **MATERIALS AND METHODS**

372 **Strains and growth conditions**

373 The strains and plasmids used in this study are listed in the supplementary table (S1)
374 and (S2). The *E. coli* strains used in this study are BW25113 and DH10B. All the *A.*
375 *tumefaciens* strains were cultured on 523 medium [47] at 28 °C unless stated. The *E. coli*
376 strains were cultured on Luria Bertani (LB) medium (10 g L−1 NaCl, 10 g L−1 tryptone,
377 and 5 g L−1 yeast extract) at 37°C unless stated. Where appropriate, the media were
378 supplemented with 100 μg mL^{-1} spectinomycin, gentamycin 25 μg mL^{-1} (for *E. coli*) and
379 50 μg mL^{-1} (for *A. tumefaciens*), 50 μg mL^{-1} ampicillin, 50 μg mL^{-1} kanamycin, 1 mM
380 Isopropyl β- d-1-thiogalactopyranoside (IPTG).

381 **Growth inhibition assay**

382 For growth inhibition assay of IPTG-inducible expression of Tde1 and its variants, *E. coli*
383 (DH10B) harbouring pTrc200 vector or the derivatives expressing Tde1 variants were
384 grown overnight in LB medium supplemented with spectinomycin prior to 1:30 dilution in
385 a fresh medium and incubated for 2 hrs at 37°C with 250 rpm. After 2 hrs, the cultures
386 were normalized to OD_{600} 0.1 in LB with 1 mM IPTG for continuous culture in the same
387 growth condition. The growth of *E. coli* was monitored for OD_{600} every one hr using
388 ULTROSPEC® 10 cell density meter (Biochrom, UK). For growth inhibition assay of
389 arabinose-inducible expression, *E. coli* BW25113 harbouring pJN105 vector or the
390 derivatives expressing Tde1 variants were used. Overnight cultures of *E. coli* cells were
391 adjusted to an OD_{600} of 0.1 in 200 µL LB with 0.2% L-arabinose in a 96-well plate. The
392 OD_{600} values were measured by the Synergy H1 microplate reader (Agilent
393 Technologies, USA) with agitation at 37 °C. The OD_{600} values of final time points were
394 used to calculate mean ± SD of three repeats. One way Analysis of Variance (ANOVA)
395 was used for the analysis of statistical significance followed by the Tukey's multiple
396 comparison.

397 ***In vivo* plasmid DNA degradation assay.** The *in vivo* plasmid DNA degradation assay
398 was performed as described [23] with minor modifications. Briefly, overnight cultures of *E.*
399 *coli* BW25113 carrying pJN105 vector or the derivatives expressing Tde1 variants were
400 adjusted to an OD_{600} of 0.3 in 4 mL LB with 0.5% D-glucose or 0.2% L-arabinose. After
401 induction for 3 hrs, bacterial cells normalized by OD_{600} were collected for plasmid DNA
402 extraction and western blot analysis. The plasmids were then extracted and applied to
403 0.6% agarose gel electrophoresis to detect the DNA degradation. The OD_{600} values
404 were measured by DEN-600 photometer (Biosan, Latvia) every hr.

405 **β-galactosidase and viability assays for ONPG update**

406 β-galactosidase assay was performed as described [48] with minor modifications.
407 BW25113 wild type, BW25113Δ*lacY*(pYTA-lacZ), or BW25113Δ*lacY* harbouring
408 pTrc200 vector or the derivatives expressing Tde1 variants were grown overnight and
409 refreshed to a fresh medium as stated for growth inhibition assay. After subculture for 2
410 hrs, the cells were induced with 1 mM IPTG, and incubated for one more hr. Part of the
411 culture was adjusted to OD_{600} = 0.3 in Z-buffer and the Intracellular β-galactosidase

412 activity was measured by mixing 100 µl of 4 mg/ml ONPG with 900 µL of the cells and
413 incubation at room temperature for 10 mins prior to measurement at OD_{420}. The
414 remaining cells were normalized to OD_{600} 0.3 in 0.9 % sterile saline and after serial
415 dilution, 10 µL was spotted on LB plate without antibiotics to recover the viable cells.
416 Data of OD_{420} were used to calculate mean ± SD of three independent experiments.
417 One way ANOVA was used for the analysis of statistical significance followed by the
418 Tukey's multiple comparison.

419 **Co-immunoprecipitation**

420 The Co-immunoprecipitation (co-IP) was performed according to the manufacturer's
421 recommendations of EZview red Anti-HA agarose (Sigma-E6779) with minor
422 modifications. To identify Tap1 interacting domain of Tde1, the HA tagged Tde1 variants
423 were expressed on pTrc200 plasmid. For co-IP in *A. tumefaciens,* C58 Δ*tde1* cells
424 expressing the Tde1 variants grown in 523 medium overnight were resuspended in a 1:30
425 ratio to a fresh medium and incubated at 25°C for 3 hrs followed by 1 mM IPTG induction
426 for additional 3 hrs. After 6 hrs post incubation, the cells were normalized to OD_{600} of 5
427 per mL in ice-cold PBS buffer (pH 7.4). After cell lysis by lysozyme treatment and
428 sonication, the lysate was centrifuged and a 100 µL aliquot of the lysate was saved for
429 the input fraction. The remaining 900 µL lysate was mixed with 25 µL of pre-equilibrated
430 EZview red Anti-HA agarose and incubated at 4 °C for 1 hr. The beads were then washed
431 3 times with ice-cold PBS buffer and the proteins bound to the beads were eluted with
432 100 µL of 2X SDS sample loading buffer. Similarly, the aliquoted input fraction was mixed
433 with equal volume of 2X SDS sample loading buffer for analysis by western blotting.

434 For Co-IP in *E. coli*, the HA tagged Tde1 variants were expressed in DH10B cells from
435 pTrc200 plasmid and Tap1 was expressed from pRL662 plasmid. Overnight culture was
436 resuspended to fresh medium with 1:30 ratio and incubated for two hrs, followed by
437 induction with 1 mM IPTG and incubated at 37°C with 250 rpm for two hrs. The cells were
438 lysed followed by co-IP as stated earlier.

439 **Secretion assay**

440 Type VI Secretion assay was performed in 523 as described previously [32]. Briefly, *A.*
441 *tumefaciens* strain was cultured overnight in 523 medium and normalized to OD_{600} of 0.2
442 in a fresh medium. After 6 hrs of culture, the secreted proteins were collected by
443 centrifuging at 10,000 g for 5 mins. The resulting pellet was adjusted to OD_{600} of 10 as a
444 cellular fraction. The culture supernatant was filtered with 0.22 µm Millipore filter
445 membrane and resulting filtrate was subjected for TCA precipitation [49] and referred as an
446 extracellular fraction.

447 **Western blotting**

448 Western blot analyses were done as previously described [50]. The following primary
449 antibody titres used were: HA epitope (1:4,000), Tap1 (1:3,000) [50], Strep (1:4,000), EF-
450 Tu (1:6,000), and C-terminal Tde1 (1:4,000) [23,28], Hcp (1:2,500) [49].

451 **Interbacterial competition assays**

452 For interbacterial competition with *E. coli* (target), *A. tumefaciens* strain (attacker) was
453 grown overnight at 28°C in 523 broth with appropriate antibiotics if needed. *E. coli* DH10B
454 harbouring pRL662 plasmid was grown at 37°C in LB broth with gentamycin. After
455 harvesting and washing the cells in 0.9% saline, the attacker to target cell density was
456 adjusted to 30:1 (OD_{600} =3: 0.1) and the mix was spotted on Agrobacterium kill-triggering
457 (AK) medium containing 1.5% (wt/vol) agar [24]. Similar procedure is used when using *A.*
458 *tumefaciens* strain 1D1609 as a target, which was grown at 28°C in 523 broth prior to
459 competition. After incubation of the mixed strains for 16 hrs at 28°C, the surviving cells
460 were selected on a gentamycin-containing LB agar square plate.

461 **Fluorescence microscopy**

462 For propidium iodide and Hoechst staining, *E. coli* cells (BW25113) harbouring Trc200
463 vector or derivatives expressing Tde1 variants were grown overnight and refreshed to a
464 fresh medium as stated for growth inhibition assay. After subculture for 2 hrs, the cells
465 were induced with 1 mM IPTG for one hr and OD_{600} equivalent to 0.3 was collected in 1
466 ml PBS and stained with Hoechst 33342 (H3570) to a final concentration of 12.3 µg/mL
467 and 1 µg/ml Propidium iodide (2208511) and incubated for 2 minutes in dark. Finally, 2
468 µL was spotted on 2.5% agarose pad.

469 For the translocation experiment, the sfGFP fused Tde1 variants were expressed in *A.*
470 *tumefaciens* Δ*tdei* cells (attacker). *E. coli* (target) cells were labelled with mCherry (false
471 colour blue) expressed from pBBRMCS2. *A. tumefaciens* attacker cells were cultured in
472 523 broth overnight, and *E. coli* target cells were separately cultured on LB broth.
473 Overnight cultured attacker and target cells were mixed at 5:1 ratio (OD_{600}= 1.0: 0.2), and
474 10 µL of the mix was cultured on LB-agar plate without IPTG. After 20 hrs of co-culture,
475 the cells were washed with 100 µL PBS and 2 µL of suspension was spotted on the 2.5%
476 agarose pad on a microscopic slide. The merged GFP and mCherry signals was based
477 on a cyan fluorescence.

478 Fluorescence microscopy was performed using Axio Observer 7 (Zeiss, Germany)
479 microscope equipped with an Axiochem 702 digital camera and a Plan-Apochromat
480 100x/1.4 Oil DIC H objective. Exposure times were adjusted to 20 ms for Phase, 20 ms
481 for Hoechst, 150 ms for PI, 200 ms for GFP and 5000 ms for mCherry. Multiple images
482 were taken from different fields and all the experiments were performed at least in
483 triplicate and a representative image is shown. Images were analyzed by using ZEN 2.3
484 (blue edition) software.
485

486 **Domain prediction and analysis**

487 Full-length Tde1 (1-278) was used as a query for conserved domain search on the
488 conserved domains database (CDD) [51] of the National Center for Biotechnology
489 Information (NCBI). Prediction of transmembrane domain was done using the PRED-
490 TMR2 [52]. The Tde1 homologues and tape measure proteins (TMPs) for the multiple
491 sequence alignment were obtained by BLAST search of N-Tde1 (1-97) against the
492 NCBI non redundant database (nr) with representative sequences selected for multiple
493 sequence alignment. The domain architectures of the Ntox15 domain containing
494 proteins were obtained using the full length Tde1 against Conserved Domain
495 Architectural retrieval tool (CDART) of NCBI. The information of gene clusters encoding
496 Tde1 homologues and TMPs including upstream and downstream three genes was
497 retrieved from their respective genomes. Full-length Tde1 (1-278) was used as a query
498 for structural prediction on a Phyre2 [53]. Three-dimensional structure modelling was done

499 using Phyre2 in intensive modelling mode. Crystal structure served as best template for
500 the N-terminus and percentage of confidence for three-dimensional structure modelling
501 are indicated in the legends of corresponding figures. The structural graphics were
502 generated by using ChimeraX 1.1 [54].

503

504 **ACKNOWLEDGEMENT**

505 We would like to thank the Lai lab members for their help and fruitful discussion
506 throughout this study, Yun-Wei Lien for generating the Δ*tdei*Δ*tssK* strain, and Chih-
507 Horng Kuo for discussion and suggestion on BLAST analysis. The authors highly
508 appreciate Jeff Chang, See-Yeun Ting, Lay-Sun Ma, and Chih-Feng Wu for critically
509 reading the manuscript and their valuable comments. We also acknowledge the
510 technical assistance of fluorescence microscope provided by Mei-Jane Fang from Live
511 Cell Imaging Division of Cell Biology Core and Sanger DNA sequencing service
512 provided by Genomic Technology Core, both located at the Institute of Plant and
513 Microbial Biology, Academia Sinica. The authors also thank Ying Wang for illustration of
514 proposed model. The funding was supported by Ministry of Science and Technology of
515 Taiwan (MOST 110-2311-B-001-032-MY3) and Academia Sinica Investigator Award
516 (AS-IA-107-L01) to EML. YWC was supported by the postdoctoral fellowship (MOST
517 110-2811-B-001-524). The funders had no role in study design, data collection and
518 interpretation, or the decision to submit the work for publication.

519 **AUTHOR CONTRIBUTION**

520 Conceptualization: JA, MY, EML; Investigation: JA, MY, LKS, YWC; Project Funding
521 acquisition and administration: EML; Supervision: EML; Writing of original draft: JA,
522 EML; Writing – methodology, review & editing: JA, MY, LKS, YWC, EML.

523

524 **FIGURE LEGENDS**

525 **Figure 1. Schematic domain organization, sequence alignment, growth inhibition**
526 **assay. (**A) Schematic domain organization of Tde1 protein and its variants. The N-

527 terminal repeated glycine zipper motifs (12-51) overlapping a predicted transmembrane
528 domain (22-42) and Ntox15 DNase domain (99-247) are indicated. Tde1 and its variants
529 with truncation or amino acid substitutions were illustrated. (B) Growth inhibition assay of
530 *E. coli* DH10B cells harbouring pTrc200 vector or each of its derivatives expressing Tde1
531 variants with IPTG induction. (C) Growth inhibition assay of *E. coli* DH10B cells co-
532 expressing the Tde1 variants expressed from pTrc200 plasmid and Tdi1 immunity gene
533 expressed from pRL662 plasmid. Growth curve was determined at $OD_{600.}$ Graphs of
534 panels B and C show mean ± SD of three independent experiments. The significant
535 differences were shown by the different letters (p value <0.01). (D) Multiple sequence
536 alignment of N-Tde1 homologues were presented with highly conserved amino acid
537 residues highlighted in yellow. The bacterial species, strain name, and locus number of
538 Tde1 orthologs (*Agrobacterium/Rhizobium*) or tape measure proteins
539 (*Paraburkholderia/Burkholderia*) are indicated on the left and right of aligned sequences.
540 Two conserved glycine residues (G^{39}, G^{43}) subjected for mutagenesis were indicated by
541 the arrows above the sequences.

542

543 **Figure 2. Membrane permeabilization assays**. (A) Growth inhibition assay of *E. coli*
544 DH10B cells harbouring pTrc200 vector or each of its derivatives expressing Tde1
545 variants with IPTG inducible expression. BW25113 WT or BW25113 (Δ*lacY)* cells
546 harbouring pTrc200 vector or each of its derivatives expressing Tde1 variants were
547 carried out for (B) β-galactosidase activity assay to determine ONPG uptake, (C)
548 propidium iodide permeability with cells treated with Propidium iodide and Hoechst for
549 detection by fluorescence microscope, and (D) viability assay for *E. coli* cells derived from
550 the ONPG uptake assay. (E) Bacteriostatic activity assay. *E. coli* DH10B cells harbouring
551 pTrc200 vector or each of its derivatives expressing Tde1 variants were cultured with or
552 without IPTG induction for 1 hr. The IPTG-induced cells were further centrifuged and
553 resuspended in the fresh medium with or without IPTG. Cell density was measured again
554 before continuous growth for additional 1 hr. Graphs of panels A, B, and E show mean ±
555 SD of three independent experiments. The significant differences were shown by the

556 different letters (p value <0.01). Panels C and D are representative results of three
557 independent experiments.

558

559 **Figure 3. The N-terminus of Tde1 is sufficient for interaction with Tap1. (**A) Co-
560 immunoprecipitation (Co-IP) in *A. tumefaciens. A. tumefaciens* C58 Δ*tde1* harbouring
561 pTrc200 vector or its derivatives expressing HA-tagged Tde1 variants. Anti-HA resin was
562 used to co-IP the Tde1 variants and Tap1. (B) Co-IP in *E. coli* DH10B. DH10B cells co-
563 expressing HA-tagged Tde1 variants from pTrc200 and Tap1 from pRL662 were collected
564 for co-IP. Anti-HA resin was used to co-IP the Tde1 variants and Tap-1. Representative
565 western blot results of three independent experiments were shown with antibody against
566 HA for Tde1 variants and Tap1 respectively. (C). Secretion assay for HA-tagged Tde1
567 variants. Western blot for the cellular and extracellular fractions of *A. tumefaciens* C58
568 Δ*tdei* and Δ*tdei1*Δ*tssK* expressing the HA-tagged Tde1 variants. Hcp secretion was
569 detected as a positive control for active T6SS secretion. Representative western blot
570 results of three independent experiments were shown with antibody against HA, Hcp, or
571 EF-Tu serving as a loading and non-secreted protein control. Protein markers are
572 indicated in kDa.

573

574 **Figure 4. The roles of N-Tde1 and $G^{39}xxxG^{43}$ glycine zipper motif for secretion and**
575 **translocation. (**A) Secretion assay for Tde1 variants fused with sfGFP. Western blot for
576 the cellular and extracellular fractions of *A. tumefaciens* C58 Δ*tdei* and Δ*tdei1*Δ*tssK*
577 expressing the Tde1 variants fused with sfGFP were detected by anti-GFP antibody.
578 Representative western blot results of three independent experiments were shown with
579 antibody against GFP, Hcp, or EF-Tu serving as a loading and non-secreted protein
580 control. Hcp secretion served as a positive control for active T6SS secretion. Protein
581 markers are indicated in kDa. (B) Fluorescence microscopy for Tde1 translocation. *A.*
582 *tumefaciens* C58 Δ*tdei* expressing Tde1 variants fused with sfGFP (in green) and *E. coli*
583 DH10B carrying mCherry (false coloured in blue) were co-cultured for 20 hrs. A cyan
584 fluorescence with merged blue and green signals represented the translocation of Tde1
585 variants from *A. tumefaciens* to *E. coli*.

586

587 **Figure 5. $G^{39}xxxG^{43}$ glycine zipper motif of Tde1 is required for DNase-mediated**
588 **killing of target cells during interbacterial competition. (**A) Inter-species
589 Interbacterial competition. *A. tumefaciens* C58 Δ*tdei* and Δ*tdei1*Δ*tssK* expressing the
590 Tde1 variants were co-incubated with *E. coli* (DH10B) cells on AK medium followed by
591 selecting target cell survival with serial dilution on a gentamycin containing LB agar at
592 37°C. (B) Intra-species Interbacterial competition between *A. tumefaciens* C58 *(*Δ*tdei)*
593 and Δ*tdei1*Δ*tssK* expressing the Tde1 variants and *A. tumefaciens* 1D1609 target cell.
594 The competition was done as in (B) except 1D1609 was recovered at 28°C. (C)
595 Secretion assay for Tde1 and its variants co-expressed with its immunity protein Tdi1.
596 The toxin immunity pairs Tde1-Tdi1, $Tde1^{GLGL}$-Tdi1, and Tde1(M)-Tdi1 were expressed
597 in *A. tumefaciens* C58 Δ*tdei* and Δ*tdei*Δ*tssK.* (D) *In vivo* plasmid DNA degradation
598 assay. *E. coli* BW25113 carrying pJN105 empty vector or the derivatives expressing
599 different variants of Tde1 were supplemented with 0.5% glucose ("-") or 0.2% L-
600 arabinose ("+") for 3 hrs to either repress or induce Tde1 production. The plasmids were
601 then extracted to observe the DNA degradation and bottom panel showed western blots
602 of specific Tde1 protein bands indicated by arrows. (E) Growth inhibition assay of Tde1
603 and its variants. *E. coli* BW25113 cells were induced by adding 0.2% L-arabinose for
604 Tde1 production. The OD_{600} values were measured every 15 minutes. The OD_{600} values
605 of the 4 h post L-arabinose induction were analysed for statistical analysis. Graphs
606 show mean ± SD of three biological repeats. The significant differences were shown by
607 the different letters (p value <0.01). All data were shown with representative results of
608 three independent experiments. Western blots were detected with specific antibody
609 against Tde1, Hcp, or EF-Tu serving as a loading and non-secreted protein control.
610 Protein markers are indicated in kDa.

611

612 **Figure 6. Proposed model of the loading, firing, and translocation of Tde1.** The Tde1
613 translocation is proposed through six steps. Step 1: Tde1 forms a complex with Tdi1 and
614 Tap1 in the attacker cell. Step 2: Tap1-Tde1-Tdi1 complex binds to the VgrG and the
615 Hcp-VgrG-PAAR puncturing device carrying Tde1 effector complex is loaded onto

membrane-associated baseplate. Step 3: Hcp tube and TssB/C sheath polymerize on the Tde1-loaded VgrG/baseplate while Tdi1 and Tap1 fall off with unknown mechanisms before or upon firing. Step 4: TssBC sheath contracts and ejects Tde1 into the target cell periplasm or cytoplasm. Step 5: The glycine zipper(s) on the N-terminus of Tde1 permeabilize the target cell membrane. Step 6: Intact or truncated Tde1 proteins attack DNA for degradation in the target cell.

Figure S1. Domain architecture and genetic organizations of Tde homologues. (A) Domain organization of the Ntox15-containing proteins. Top 10 classes of the Ntox15-containing proteins are shown with the identifiable domains (not to scale). The number of proteins in each class were indicated on the left based on the information on June 29, 2022. The *A. tumefaciens* Tde1 belonged to the first class where the N-terminal region lacks an identifiable domain. (B) Genetic organizations of genes encoding Tde1 orthologues and Tape Measure Proteins (TMPs) with sequence similarity to N-terminus of Tde1. The proteins encoded from the upstream and downstream of *tde1* and *tmp* genes are shown with their identified domain organizations.

Figure S2. Growth inhibition assays in *A. tumefaciens* and *E. coli*. Growth curve (A) and western blot analyses (B) of *A. tumefaciens* C58 Δ*tde1* carrying pTrc200 or its derivatives expressing HA-tagged Tde1 variants. The growth curve was detected every 2 hrs in 523 medium supplemented with 1 mM IPTG. Graphs show mean ± SD of three independent experiments. The significant differences were shown by the different letters (p value <0.01). The proteins collected at end point (6 hr) were analysed for western blotting with antibody against HA. Representative results of three independent experiments were shown. Protein markers are indicated in kDa. (C) The growth curve analysis of *E. coli* cells used for *in vivo* plasmid DNA degradation assay. The turbidity of *E. coli* BW25113 expressing Tde1 and its variants carried out for the *in vivo* plasmid DNA degradation assay were measured. The *E. coli* cells were supplemented with 0.5% glucose (glu) or 0.2% L-arabinose (ara) for the repression or induction of Tde1 and its

645 variants. The OD_{600} values were measured by DEN-600 photometer (Biosan, Latvia)
646 every hr.

647

648 **Figure S3. Fluorescence microscopy for negative controls of translocation assay.**
649 *A. tumefaciens* C58 Δ*tdei*Δ*tssK* expressing N-Tde1-sfGFP or Tde1(M)-sfGFP (in green)
650 and *E. coli* DH10B carrying mCherry (false coloured in blue) were co-cultured for 20 hrs.
651 No cyan fluorescence with merged blue and green signals could be detected when
652 attacker cells are T6SS-inactive, which served as negative controls for the translocation
653 assay.

654

655 **Figure S4. Structural prediction of the Tde1 N-terminus with similarity to pyocin S5**
656 **and colicins**. (A) Predicted results of N-terminal Tde1 (1-97) as a query. (B) N-terminal
657 Tde1 with structural similarity to pore-forming domain of the pyocin S5, colicines and other
658 membrane perturbing proteins based on Phyre2 prediction. (C) Cartoon model of the
659 Tde1 (residue 10 – 62) by using on the basis of the crystal structure of Pyocin S5 (PDB
660 6THK) with 77.3% of identity. Glycine residues of Tde1 were indicated. (D)
661 Superimposition of N-Tde1 and pore-forming domain of pyocin S5. Tde1 N-terminus is
662 in red and partially pore-forming domain of pyocin S5 is in teal, G^{39} and G^{43} in the putative
663 glycine zipper motif are highlighted in green. All data were analyzed by Phyre2 server.

664

665

666 **REFERENCES**

667 1 Costa, T. R. *et al.* Secretion systems in Gram-negative bacteria: structural and mechanistic insights.
668 *Nat Rev Microbiol* **13**, 343-359, doi:10.1038/nrmicro3456 (2015).
669 2 Christie, P. J. The Rich Tapestry of Bacterial Protein Translocation Systems. *Protein J* **38**, 389-408,
670 doi:10.1007/s10930-019-09862-3 (2019).
671 3 Palmer, T., Finney, A. J., Saha, C. K., Atkinson, G. C. & Sargent, F. A holin/peptidoglycan hydrolase-
672 dependent protein secretion system. *Mol Microbiol*, doi:10.1111/mmi.14599 (2020).
673 4 Coulthurst, S. The Type VI secretion system: a versatile bacterial weapon. *Microbiology (Reading)*
674 **165**, 503-515, doi:10.1099/mic.0.000789 (2019).
675 5 Russell, A. B., Peterson, S. B. & Mougous, J. D. Type VI secretion system effectors: poisons with a
676 purpose. *Nat Rev Microbiol* **12**, 137-148, doi:10.1038/nrmicro3185 (2014).
677 6 Lien, Y. W. & Lai, E. M. Type VI Secretion Effectors: Methodologies and Biology. *Front Cell Infect*
678 *Microbiol* **7**, 254, doi:10.3389/fcimb.2017.00254 (2017).
679 7 Hachani, A., Wood, T. E. & Filloux, A. Type VI secretion and anti-host effectors. *Curr Opin Microbiol*
680 **29**, 81-93, doi:10.1016/j.mib.2015.11.006 (2016).

681 8 Jurenas, D. & Journet, L. Activity, delivery, and diversity of Type VI secretion effectors. *Mol*
682 *Microbiol*, doi:10.1111/mmi.14648 (2020).
683 9 Cherrak, Y., Flaugnatti, N., Durand, E., Journet, L. & Cascales, E. Structure and Activity of the Type
684 VI Secretion System. *Microbiol Spectr* **7**, doi:10.1128/microbiolspec.PSIB-0031-2019 (2019).
685 10 Wang, J., Brodmann, M. & Basler, M. Assembly and Subcellular Localization of Bacterial Type VI
686 Secretion Systems. *Annu Rev Microbiol* **73**, 621-638, doi:10.1146/annurev-micro-020518-115420
687 (2019).
688 11 Durand, E. *et al.* Biogenesis and structure of a type VI secretion membrane core complex. *Nature*
689 **523**, 555-560, doi:10.1038/nature14667 (2015).
690 12 Cherrak, Y. *et al.* Biogenesis and structure of a type VI secretion baseplate. *Nat Microbiol* **3**, 1404-
691 1416, doi:10.1038/s41564-018-0260-1 (2018).
692 13 Zoued, A. *et al.* Priming and polymerization of a bacterial contractile tail structure. *Nature* **531**,
693 59-63, doi:10.1038/nature17182 (2016).
694 14 Basler, M., Pilhofer, M., Henderson, G. P., Jensen, G. J. & Mekalanos, J. J. Type VI secretion requires
695 a dynamic contractile phage tail-like structure. *Nature* **483**, 182-186, doi:nature10846 (2012).
696 15 Vettiger, A. & Basler, M. Type VI Secretion System Substrates Are Transferred and Reused among
697 Sister Cells. *Cell* **167**, 99-110 e112, doi:10.1016/j.cell.2016.08.023 (2016).
698 16 Cianfanelli, F. R., Monlezun, L. & Coulthurst, S. J. Aim, Load, Fire: The Type VI Secretion System, a
699 Bacterial Nanoweapon. *Trends Microbiol* **24**, 51-62, doi:10.1016/j.tim.2015.10.005 (2016).
700 17 Kim, S. *et al.* Transmembrane glycine zippers: physiological and pathological roles in membrane
701 proteins. *Proc Natl Acad Sci U S A* **102**, 14278-14283, doi:10.1073/pnas.0501234102 (2005).
702 18 Fonte, V. *et al.* A glycine zipper motif mediates the formation of toxic beta-amyloid oligomers in
703 vitro and in vivo. *Mol Neurodegener* **6**, 61, doi:10.1186/1750-1326-6-61 (2011).
704 19 Kim, S., Chamberlain, A. K. & Bowie, J. U. Membrane channel structure of *Helicobacter pylori*
705 vacuolating toxin: role of multiple GXXXG motifs in cylindrical channels. *Proc Natl Acad Sci U S A*
706 **101**, 5988-5991, doi:10.1073/pnas.0308694101 (2004).
707 20 McClain, M. S. *et al.* Essential role of a GXXXG motif for membrane channel formation by
708 *Helicobacter pylori* vacuolating toxin. *J Biol Chem* **278**, 12101-12108,
709 doi:10.1074/jbc.M212595200 (2003).
710 21 LaCourse, K. D. *et al.* Conditional toxicity and synergy drive diversity among antibacterial effectors.
711 *Nat Microbiol* **3**, 440-446, doi:10.1038/s41564-018-0113-y (2018).
712 22 Garcia-Bayona, L., Guo, M. S. & Laub, M. T. Contact-dependent killing by *Caulobacter crescentus*
713 via cell surface-associated, glycine zipper proteins. *Elife* **6**, doi:10.7554/eLife.24869 (2017).
714 23 Ma, L. S., Hachani, A., Lin, J. S., Filloux, A. & Lai, E. M. *Agrobacterium tumefaciens* deploys a
715 superfamily of type VI secretion DNase effectors as weapons for interbacterial competition in
716 planta. *Cell Host Microbe* **16**, 94-104, doi:10.1016/j.chom.2014.06.002 (2014).
717 24 Yu, M., Wang, Y. C., Huang, C. J., Ma, L. S. & Lai, E. M. *Agrobacterium tumefaciens* Deploys a
718 Versatile Antibacterial Strategy to Increase its Competitiveness. *J Bacteriol*,
719 doi:10.1128/JB.00490-20 (2020).
720 25 Chou, L. *et al.* Modular evolution of secretion systems and virulence plasmids in a bacterial species
721 complex. *BMC Biol* **20**, 16, doi:10.1186/s12915-021-01221-y (2022).
722 26 Wu, C. F. *et al.* Diversification of the Type VI Secretion System in Agrobacteria. *mBio* **12**, e0192721,
723 doi:10.1128/mBio.01927-21 (2021).
724 27 Zhang, D., de Souza, R. F., Anantharaman, V., Iyer, L. M. & Aravind, L. Polymorphic toxin systems:
725 Comprehensive characterization of trafficking modes, processing, mechanisms of action,
726 immunity and ecology using comparative genomics. *Biol Direct* **7**, 18, doi:1745-6150-7-18 (2012).

727 28 Bondage, D. D., Lin, J. S., Ma, L. S., Kuo, C. H. & Lai, E. M. VgrG C terminus confers the type VI
728 effector transport specificity and is required for binding with PAAR and adaptor-effector complex.
729 *Proc Natl Acad Sci U S A* **113**, E3931-3940, doi:10.1073/pnas.1600428113 (2016).
730 29 Epand, R. F., Sarig, H., Mor, A. & Epand, R. M. Cell-wall interactions and the selective bacteriostatic
731 activity of a miniature oligo-acyl-lysyl. *Biophys J* **97**, 2250-2257, doi:10.1016/j.bpj.2009.08.006
732 (2009).
733 30 Casteels, P., Ampe, C., Jacobs, F. & Tempst, P. Functional and chemical characterization of
734 Hymenoptaecin, an antibacterial polypeptide that is infection-inducible in the honeybee (Apis
735 mellifera). *J Biol Chem* **268**, 7044-7054 (1993).
736 31 Baba, T. *et al.* Construction of *Escherichia coli* K-12 in-frame, single-gene knockout mutants: the
737 Keio collection. *Mol Syst Biol* **2**, 2006 0008 (2006).
738 32 Wu, C. F. *et al.* Effector loading onto the VgrG carrier activates type VI secretion system assembly.
739 *Embo Rep* **21**, doi:ARTN e47961DOI 10.15252/embr.201947961 (2020).

740 33 Santos, M. N. M. *et al.* Redundancy and Specificity of Type VI Secretion vgrG Loci in Antibacterial
741 Activity of *Agrobacterium tumefaciens* 1D1609 Strain. *Frontiers in Microbiology* **10**, doi:ARTN
742 3004 10.3389/fmicb.2019.03004 (2020).

743 34 Roessner, C. A. & Ihler, G. M. Formation of transmembrane channels in liposomes during injection
744 of lambda DNA. *J Biol Chem* **261**, 386-390 (1986).
745 35 Roessner, C. A. & Ihler, G. M. Proteinase sensitivity of bacteriophage lambda tail proteins gpJ and
746 pH in complexes with the lambda receptor. *J Bacteriol* **157**, 165-170, doi:10.1128/jb.157.1.165-
747 170.1984 (1984).
748 36 Cumby, N., Reimer, K., Mengin-Lecreulx, D., Davidson, A. R. & Maxwell, K. L. The phage tail tape
749 measure protein, an inner membrane protein and a periplasmic chaperone play connected roles
750 in the genome injection process of E. coli phage HK97. *Mol Microbiol* **96**, 437-447,
751 doi:10.1111/mmi.12918 (2015).
752 37 Quentin, D. *et al.* Mechanism of loading and translocation of type VI secretion system effector
753 Tse6. *Nat Microbiol* **3**, 1142-1152, doi:10.1038/s41564-018-0238-z (2018).
754 38 Ahmad, S. *et al.* Structural basis for effector transmembrane domain recognition by type VI
755 secretion system chaperones. *Elife* **9**, doi:10.7554/eLife.62816 (2020).
756 39 Fridman, C. M., Keppel, K., Gerlic, M., Bosis, E. & Salomon, D. A comparative genomics
757 methodology reveals a widespread family of membrane-disrupting T6SS effectors. *Nat Commun*
758 **11**, 1085, doi:10.1038/s41467-020-14951-4 (2020).
759 40 Miyata, S. T., Unterweger, D., Rudko, S. P. & Pukatzki, S. Dual expression profile of type VI
760 secretion system immunity genes protects pandemic *Vibrio cholerae*. *PLoS Pathog* **9**, e1003752,
761 doi:10.1371/journal.ppat.1003752 (2013).
762 41 Behrens, H. M. *et al.* Pyocin S5 Import into *Pseudomonas aeruginosa* Reveals a Generic Mode of
763 Bacteriocin Transport. *mBio* **11**, doi:10.1128/mBio.03230-19 (2020).
764 42 Ling, H., Saeidi, N., Rasouliha, B. H. & Chang, M. W. A predicted S-type pyocin shows a bactericidal
765 activity against clinical *Pseudomonas aeruginosa* isolates through membrane damage. *FEBS Lett*
766 **584**, 3354-3358, doi:10.1016/j.febslet.2010.06.021 (2010).
767 43 Wettstadt, S. & Filloux, A. Manipulating the type VI secretion system spike to shuttle passenger
768 proteins. *PLoS One* **15**, e0228941, doi:10.1371/journal.pone.0228941 (2020).
769 44 Wettstadt, S., Lai, E. M. & Filloux, A. Solving the Puzzle: Connecting a Heterologous *Agrobacterium*
770 *tumefaciens* T6SS Effector to a *Pseudomonas aeruginosa* Spike Complex. *Front Cell Infect*
771 *Microbiol* **10**, 291, doi:10.3389/fcimb.2020.00291 (2020).

45 Ho, B. T., Fu, Y., Dong, T. G. & Mekalanos, J. J. *Vibrio cholerae* type 6 secretion system effector trafficking in target bacterial cells. *Proc Natl Acad Sci U S A* **114**, 9427-9432, doi:10.1073/pnas.1711219114 (2017).

46 Hersch, S. J., Lam, L. & Dong, T. G. Engineered Type Six Secretion Systems Deliver Active Exogenous Effectors and Cre Recombinase. *mBio* **12**, e0111521, doi:10.1128/mBio.01115-21 (2021).

47 Kado, C. I., and Heskett, M.G. . Selective media for isolation of *Agrobacterium, Carynebacterium, Erwinia, Pseudomonas,* and *Xanthomonas*. . *Phytopathology* **60**, 969-976 (1970).

48 Saint Jean, K. D. *et al.* Effects of Hydrophobic Amino Acid Substitutions on Antimicrobial Peptide Behavior. *Probiotics Antimicrob Proteins* **10**, 408-419, doi:10.1007/s12602-017-9345-z (2018).

49 Wu, H. Y., Chung, P. C., Shih, H. W., Wen, S. R. & Lai, E. M. Secretome Analysis Uncovers an Hcp-Family Protein Secreted via a Type VI Secretion System in *Agrobacterium tumefaciens*. *J. Bacteriol* **190**, 2841-2850 (2008).

50 Lin, J. S., Ma, L. S. & Lai, E. M. Systematic Dissection of the *Agrobacterium* Type VI Secretion System Reveals Machinery and Secreted Components for Subcomplex Formation. *PLoS One* **8**, e67647, doi:10.1371/journal.pone.0067647 (2013).

51 Lu, S. *et al.* CDD/SPARCLE: the conserved domain database in 2020. *Nucleic Acids Res* **48**, D265-D268, doi:10.1093/nar/gkz991 (2020).

52 Pasquier, C., Promponas, V. J., Palaios, G. A., Hamodrakas, J. S. & Hamodrakas, S. J. A novel method for predicting transmembrane segments in proteins based on a statistical analysis of the SwissProt database: the PRED-TMR algorithm. *Protein Eng* **12**, 381-385, doi:10.1093/protein/12.5.381 (1999).

53 Kelley, L. A., Mezulis, S., Yates, C. M., Wass, M. N. & Sternberg, M. J. The Phyre2 web portal for protein modeling, prediction and analysis. *Nat Protoc* **10**, 845-858, doi:10.1038/nprot.2015.053 (2015).

54 Goddard, T. D. *et al.* UCSF ChimeraX: Meeting modern challenges in visualization and analysis. *Protein Sci* **27**, 14-25, doi:10.1002/pro.3235 (2018).

55 Ma, L. S., Lin, J. S. & Lai, E. M. An IcmF family protein, ImpLM, is an integral inner membrane protein interacting with ImpKL, and its walker a motif is required for type VI secretion system-mediated Hcp secretion in *Agrobacterium tumefaciens*. *J Bacteriol* **191**, 4316-4329, doi:JB.00029-09 (2009).

56 Schmidt-Eisenlohr, H., Domke, N. & Baron, C. TraC of IncN plasmid pKM101 associates with membranes and extracellular high-molecular-weight structures in Escherichia coli. *J Bacteriol* **181**, 5563-5571 (1999).

57 Vergunst, A. C. *et al.* VirB/D4-dependent protein translocation from *Agrobacterium* into plant cells. *Science* **290**, 979-982, doi:8951 [pii] (2000).

58 Newman, J. R. & Fuqua, C. Broad-host-range expression vectors that carry the L-arabinose-inducible *Escherichia coli araBAD* promoter and the *araC* regulator. *Gene* **227**, 197-203, doi:S0378-1119(98)00601-5 [pii] (1999).

814 **Table S1. List of Strains and plasmids**

Strain/plasmid Name	Relevant Characteristics	Source/Reference	EML No
A. tumefaciens			
C58	Wild type, virulent strain containing nopaline-type Ti plasmid pTiC58	Eugene Nester	EML530
ΔtssL	*tssL* deletion mutant	[55]	EML1073
Δtde1	Deletion of *atu4350*		
Δtdei	Deletion of *tde1-tdi1 (atu4350-atu4351)* and *tde2-tdi2 (atu3640-atu3639)* toxin immunity pairs	[23]	EML3559
ΔtdeiΔtssK	Deletion of *tssK* in *Δtdei*	This Study	EML5136
E. coli			
DH10B	F- *araDJ39 Δara, leu)7697 ΔlacX74 galU galK rpsL deoR φ80dlacZΔM15 endAI nupG recAI mcrA Δ (mrr hsdRMS mcrBC)*	Invitrogen	EML5396
BW25113	*rrnB Δ lacZ4787 hsdR514 Δ (araBAD)567 DE (rhaBAD)568 rph-1* (ME9062)	NBRP, Japan	EML5398
BW25113 (Δ*lacY*)	*lacY* deletion mutant of the BW25113	NBRP, Japan	
Plasmids			
pTrc200	Sm^R, Sp^R, pVS1 origin *lacIq*, *trc* promoter expression vector	[56]	EML5481
pRL662	Gm^R, non-conjugal transferable broad host range vector derived from pBBR1MCS-2,	[57]	EML5452
pRL662-Tap1	Constitutive expression of Tap1 on pRL662 plasmid	[23]	EML4269
pRL662-Tdi1-Strep	Constitutive expression of Tdi1-Strep by *lac* promoter on the pRL662 plasmid	[23]	EML3398
pTrc-Tde1(M)-HA	Sp^R, C-terminal HA-tagged Tde1(M) driven by *trc* promoter on pTrc200	This Study	EML5445
pRLTdi1-Strep	Gm^R, constitutive expression of C-terminal Strep-tagged Tdi1 by *lac* promoter on pRL662	This Study	EML5453
pTrc-N-Tde1-HA	Sp^R, N-terminus of Tde1 (1-49) with C-terminal HA tag driven by *trc* promoter on pTrc200	This Study	EML5482
pTrc-N-Tde1^{GLGL}-HA	Sp^R, N-terminus of Tde1 (1-49) with amino acid substitutions (G39L, G43L) and HA tag on C-terminus driven by *trc* promoter on pTrc200	This Study	EML5464
pTrc-Tde1(M)^{GLGL}-HA	Sp^R, C-terminal HA-tagged Tde1(M) with amino acid substitutions (G39L, G43L) driven by *trc* promoter on pTrc200	This study	EML5465
pTrc-C1-Tde1(M)-HA	Sp^R, C-terminus of Tde1(M) (49-278) with C-terminal HA tag driven by *trc* promoter on pTrc200.	This study	EML5479

pTrc-C2-Tde1(WT)-HA	Sp^R, C-terminus of Tde1 (98-278) with C-terminal HA tag driven by *trc* promoter on pTrc200.	This Study	EML5478
pYTA_LacZ	Amp^R, full length *lacZ* gene was cloned on to the YTA vector by TA cloning	This Study	EML1661
pBBRMCS2-mCherry	Km^R, full length mCherry gene was cloned on to pBBRMCS2 plasmid	This Study	EML3022
pTrc200-LacY	Sp^R, *lacY* from BW25113 with C-terminal HA tag driven by *trc* promoter on pTrc200 plasmid.	This Study	EML6350
pTrc-N-Tde1-sfGFP	Sp^R, N-terminus of Tde1 (1-49) fused to the sfGFP on the C-terminal with a GGGS linker driven by *trc* promoter on pTrc200 plasmid	This Study	EML5489
pTrc-N-Tde1^{GLGL}-sfGFP	Sp^R, N-terminus of Tde1 (1-49) with point mutation (G39L, G43L) fused to the sfGFP on the C-terminal with a GGGS linker driven by *trc* promoter on pTrc200 plasmid	This Study	EML5490
pTrc-Tde1(M)-sfGFP	Sp^R, full length of Tde1(M) fused to the sfGFP on the C-terminal with a GGGS linker driven by *trc* promoter on pTrc200 plasmid	This Study	EML5493
pTrc-Tde1(M)^{GLGL}-sfGFP	Sp^R, full length of Tde1(M) with point mutation on (G39L, G43L) fused to the sfGFP on the C-terminal with a GGGS linker driven by *trc* promoter on pTrc200 plasmid	This Study	EML5494
pTrc-C1-Tde1(WT)-HA	Sp^R, C-terminus of Tde1 (49-278) fused to the sfGFP on the C-terminal with a GGGS linker driven by *trc* promoter on pTrc200 plasmid	This Study	EML5492
pTrc-C2-Tde1(WT)-HA	Sp^R, C-terminus of Tde1 (98-278) fused to the sfGFP on the C-terminal with a GGGS linker driven by *trc* promoter on pTrc200 plasmid	This Study	EML5491
pTrc200-sfGFP	Sp^R, sfGFP was cloned in to the pTrc200 plasmid	This Study	EML5495
pJN105	Gm^R, arabinose-inducible gene expression vector derived from pBBRMCS-1, araC-P_{BAD}	[58]	
pJN105_Tde1	Gm^R, pJN105 expressing C-terminal 6xHis tagged Tde1	This study	
pJN105_Tde1^{G39L}	Gm^R, pJN105 expressing C-terminal 6xHis tagged Tde1 with the substitution of G39L	This study	
pJN105_Tde1^{G43L}	Gm^R, pJN105 expressing C-terminal 6xHis tagged Tde1 with the substitution of G43L	This study	
pJN105_Tde1^{GLGL}	Gm^R, pJN105 expressing C-terminal 6xHis tagged Tde1 with the substitutions of G39L and G43L	This study	
pJN105_Tde1(M)	Gm^R, pJN105 expressing C-terminal 6xHis tagged Tde1 with the substitutions of H190A and D193A	This study	

817 **Table S2. List of primers used to make constructs**

Plasmid/Construct made with the primers	Primer names and Sequence (restriction site is indicated underline)
pTrc200_sfGFP	NcoI_sfGFP_F: TGGACCCATGGACCGTAAAGGCGAAGAGCTGTTCA HindIII_sfGFP_R:TCGACAAGCTTTTTGTACAGTTCATCCATACCATG
pTrc200_Tde1(M)-HA	NCoI_Tde1_F: AAAAACCATGGACATGAGTGCGACGACAACTGTCG
pTrc200_N-Tde1-HA pTrc200_N-Tde1^{G}-HA	XbaI-Tde1_R: AAAAATCTAGACACCGGGACGTCAGGATTGCC XbaI_N-tde1_R: AAAAATCTAGA A GCT CCC TCA GGC GGA CTA AAG CAA T
pTrc200_C1Tde1(M)-HA pTrc200_C2-Tde1(M)-HA	NCoI_C2-Tde1_F: AAAAACCATGGACACGCCTAAGCAAGTTGAAGAGTTTAGG NcoI_C1_Tde1_F: AAAAACCATGGACGCGGGTAGAGCGGCTGCCTCCGCAA
pTrc200_N-Tde1^{G}-HA pTrc200_Tde1(M)^{G}-HA	G39L_G43L_F: TGGAGGTACAGCGGTTTTAGCATGGATACTTGGGCAAGTCGGCGCTAT G39L_G43L_R: ATAGCGCCGACTTGCCCAAGTATCCATGCTAAAACCGCTGTACCTCCAG
pTrc200_lacY-HA	NcoI_LacY_F: AAAAACCATGGACATGTACTATTTAAAAAACACAAAC XbaI_LacY_R: AAAAATCTAGAAGCGACTTCATTCACCTGACGAC
pTrc200_N-Tde1-sfGFP	N-tde_GGGS_sfGFP_F: TTAGTCCGCCTGAGGGAGCTTCTAGAGGTGGTGGTTCTCGTAAAGGCGAAGAGCTGTT sfGFP_GGGS_Ntde1_R: ACAGCTCTTCGCCTTTACGAGAACCACCACCTCTAGAAGCTCCCTCAGGCGGACTAA
pTrc200_sfGFP	NcoI_sfGFP_F: TGGACCCATGGACCGTAAAGGCGAAGAGCTGTTCA HindIII_sfGFP_R:TCGACAAGCTTTTTGTACAGTTCATCCATACCATG
pJN105_Tde1	pET-rbs-F1-XbaI: CCCCTCTAGAAATAATTTTGTTTAAC pET-R1-SacI: GGAAGAGCTCCCTTTCGGGCTTTGTTAG

818

819

820

Figure 1.

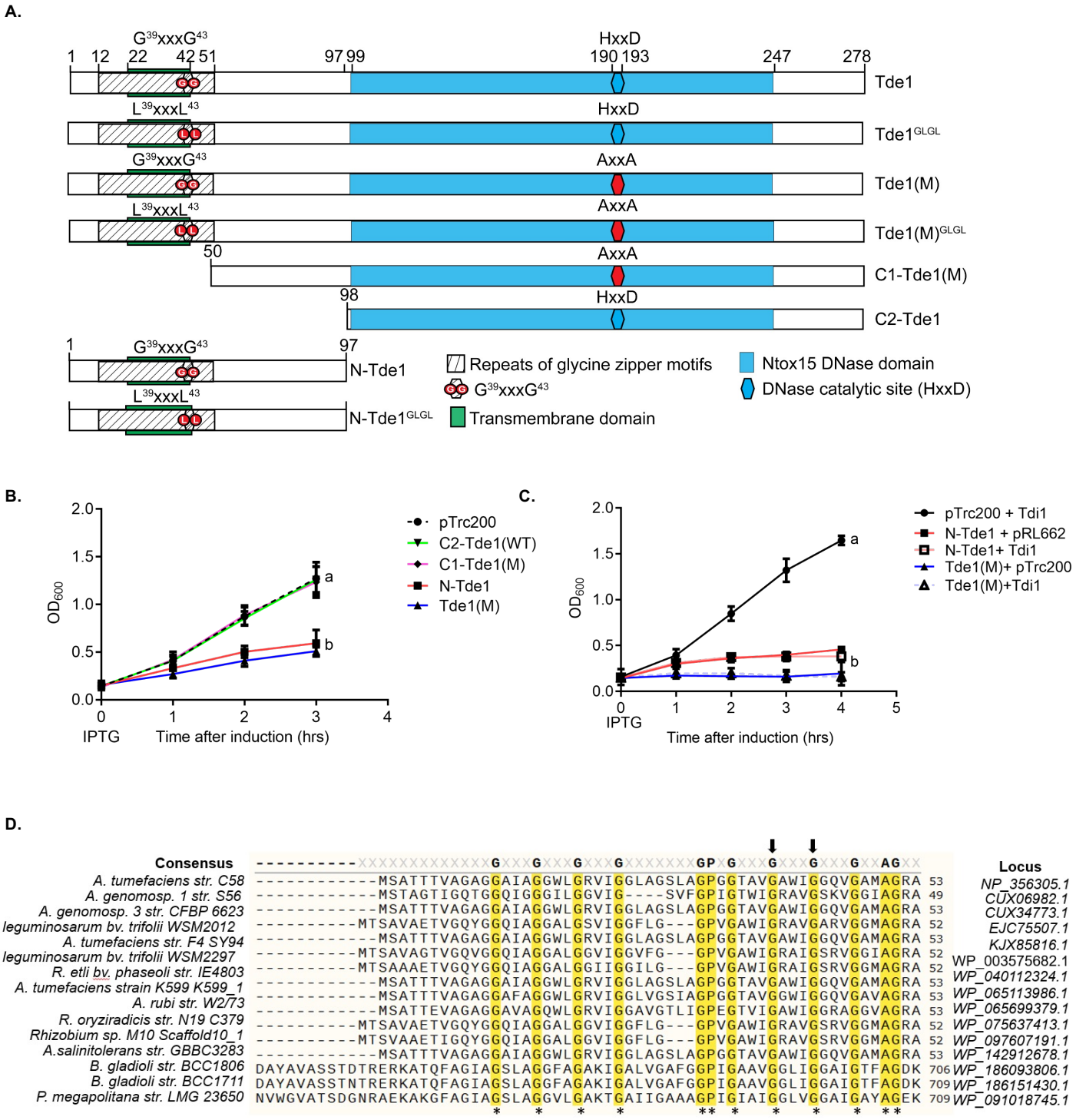

Figure 1. Schematic domain organization, sequence alignment, growth inhibition assay. (A) Schematic domain organization of Tde1 protein and its variants. The N-terminal repeated glycine zipper motifs (12-51) overlapping a predicted transmembrane domain (22-42) and Ntox15 DNase domain (99-247) are indicated. Tde1 and its variants with truncation or amino acid substitutions were illustrated. (B) Growth inhibition assay of *E. coli* DH10B cells harbouring pTrc200 vector or each of its derivatives expressing Tde1 variants with IPTG induction. (C) Growth inhibition assay of *E. coli* DH10B cells co-expressing the Tde1 variants expressed from pTrc200 plasmid and Tdi1 immunity gene expressed from pRL662 plasmid. Growth curve was determined at OD_{600}. Graphs of panels B and C show mean ± SD of three independent experiments. The significant differences were shown by the different letters (p value <0.01). (D) Multiple sequence alignment of N-Tde1 homologues were presented with highly conserved amino acid residues highlighted in yellow. The bacterial species, strain name, and locus number of Tde1 orthologs (*Agrobacterium/Rhizobium*) or tape measure proteins (*Paraburkholderia/Burkholderia*) are indicated on the left and right of aligned sequences. Two conserved glycine residues (G^{39}, G^{43}) subjected for mutagenesis were indicated by the arrows above the sequences.

Figure 2

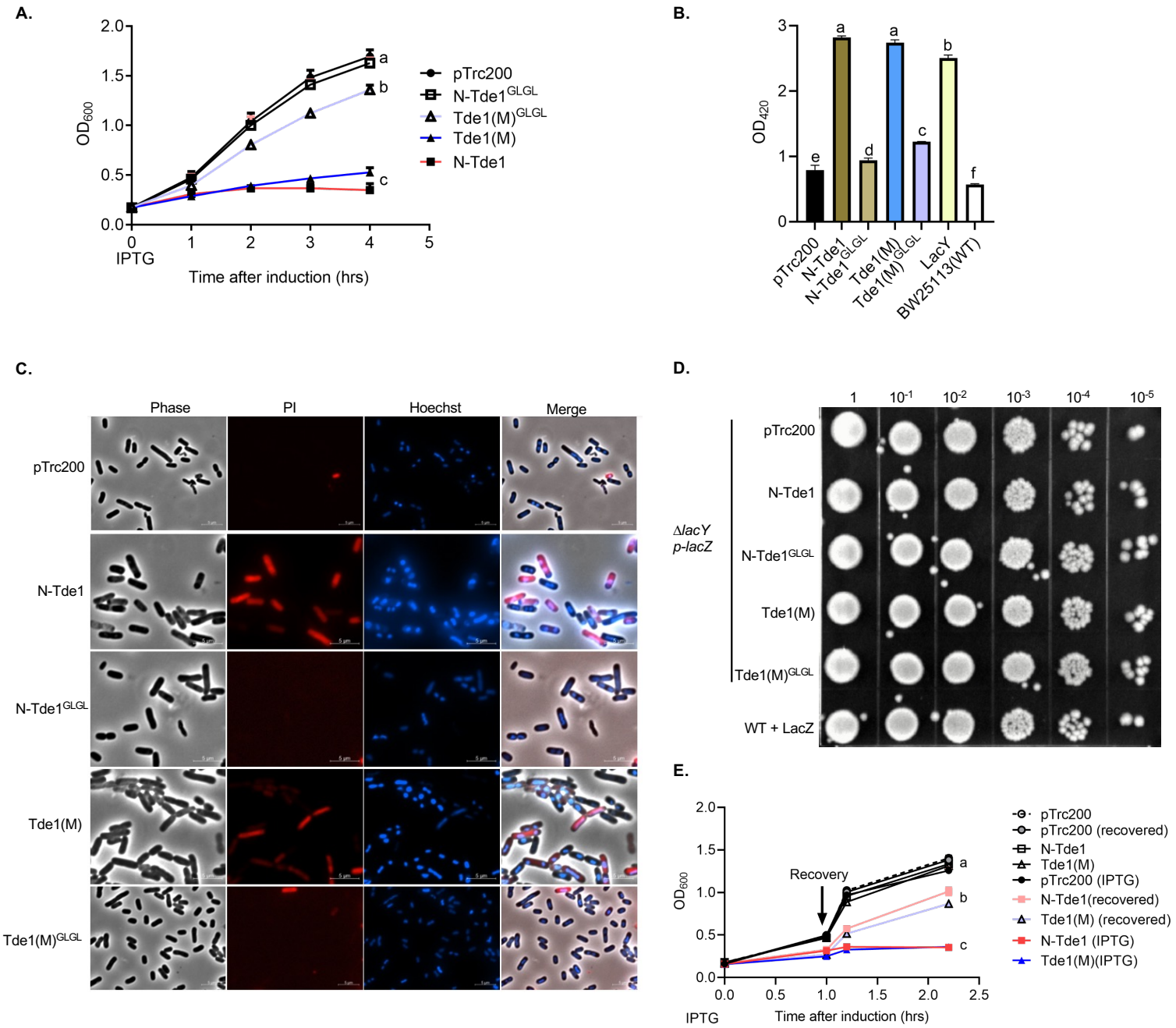

Figure 2. Membrane permeabilization assays. (A) Growth inhibition assay of *E. coli* DH10B cells harbouring pTrc200 vector or each of its derivatives expressing Tde1 variants with IPTG inducible expression. BW25113 WT or BW25113 (Δ*lacY)* cells harbouring pTrc200 vector or each of its derivatives expressing Tde1 variants were carried out for (B) β-galactosidase activity assay to determine ONPG uptake, (C) propidium iodide permeability with cells treated with Propidium iodide and Hoechst for detection by fluorescence microscope, and (D) viability assay for *E. coli* cells derived from the ONPG uptake assay. (E) Bacteriostatic activity assay. *E. coli* DH10B cells harbouring pTrc200 vector or each of its derivatives expressing Tde1 variants were cultured with or without IPTG induction for 1 hr. The IPTG-induced cells were further centrifuged and resuspended in the fresh medium with or without IPTG. Cell density was measured again before continuous growth for additional 1 hr. Graphs of panels A, B, and E show mean ± SD of three independent experiments. The significant differences were shown by the different letters (p value <0.01). Panels C and D are representative results of three independent experiments.

Figure 3

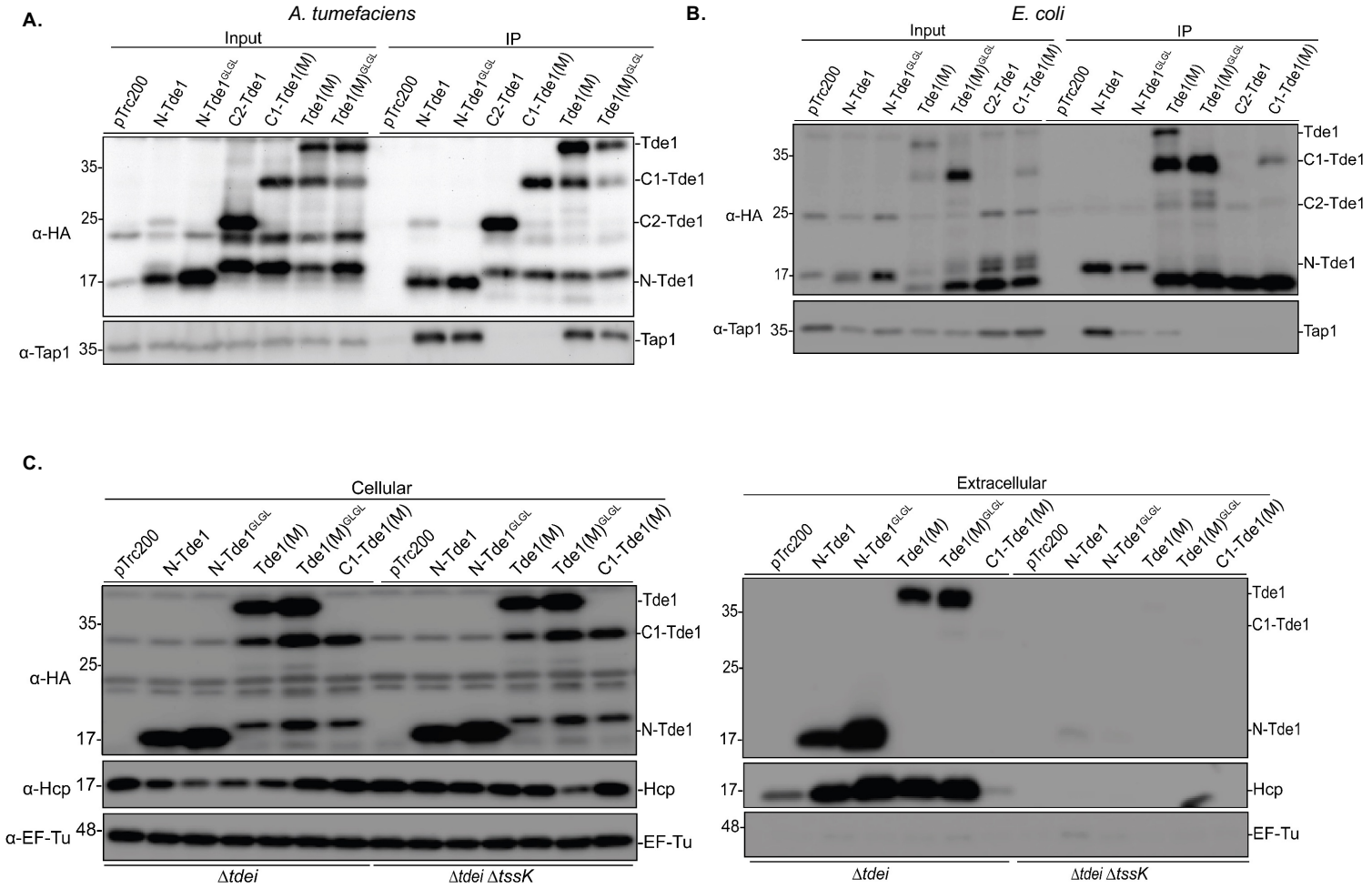

Figure 3. The N-terminus of Tde1 is sufficient for interaction with Tap1. (A) Co-immunoprecipitation (Co-IP) in *A. tumefaciens. A. tumefaciens* C58 Δ*tde1* harbouring pTrc200 vector or its derivatives expressing HA-tagged Tde1 variants. Anti-HA resin was used to co-IP the Tde1 variants and Tap1. (B) Co-IP in *E. coli* DH10B. DH10B cells co-expressing HA-tagged Tde1 variants from pTrc200 and Tap1 from pRL662 were collected for co-IP. Anti-HA resin was used to co-IP the Tde1 variants and Tap-1. Representative western blot results of three independent experiments were shown with antibody against HA for Tde1 variants and Tap1 respectively. (C). Secretion assay for HA-tagged Tde1 variants. Western blot for the cellular and extracellular fractions of *A. tumefaciens* C58 Δ*tdei* and Δ*tdei1*Δ*tssK* expressing the HA-tagged Tde1 variants. Hcp secretion was detected as a positive control for active T6SS secretion. Representative western blot results of three independent experiments were shown with antibody against HA, Hcp, or EF-Tu serving as a loading and non-secreted protein control. Protein markers are indicated in kDa.

Figure 4

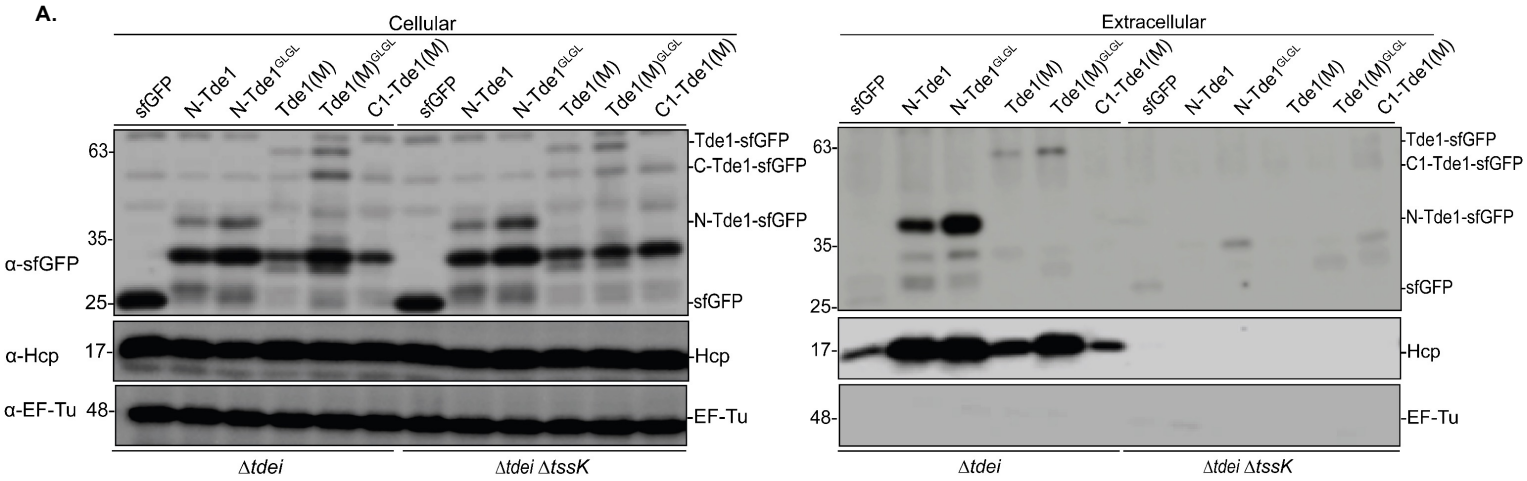

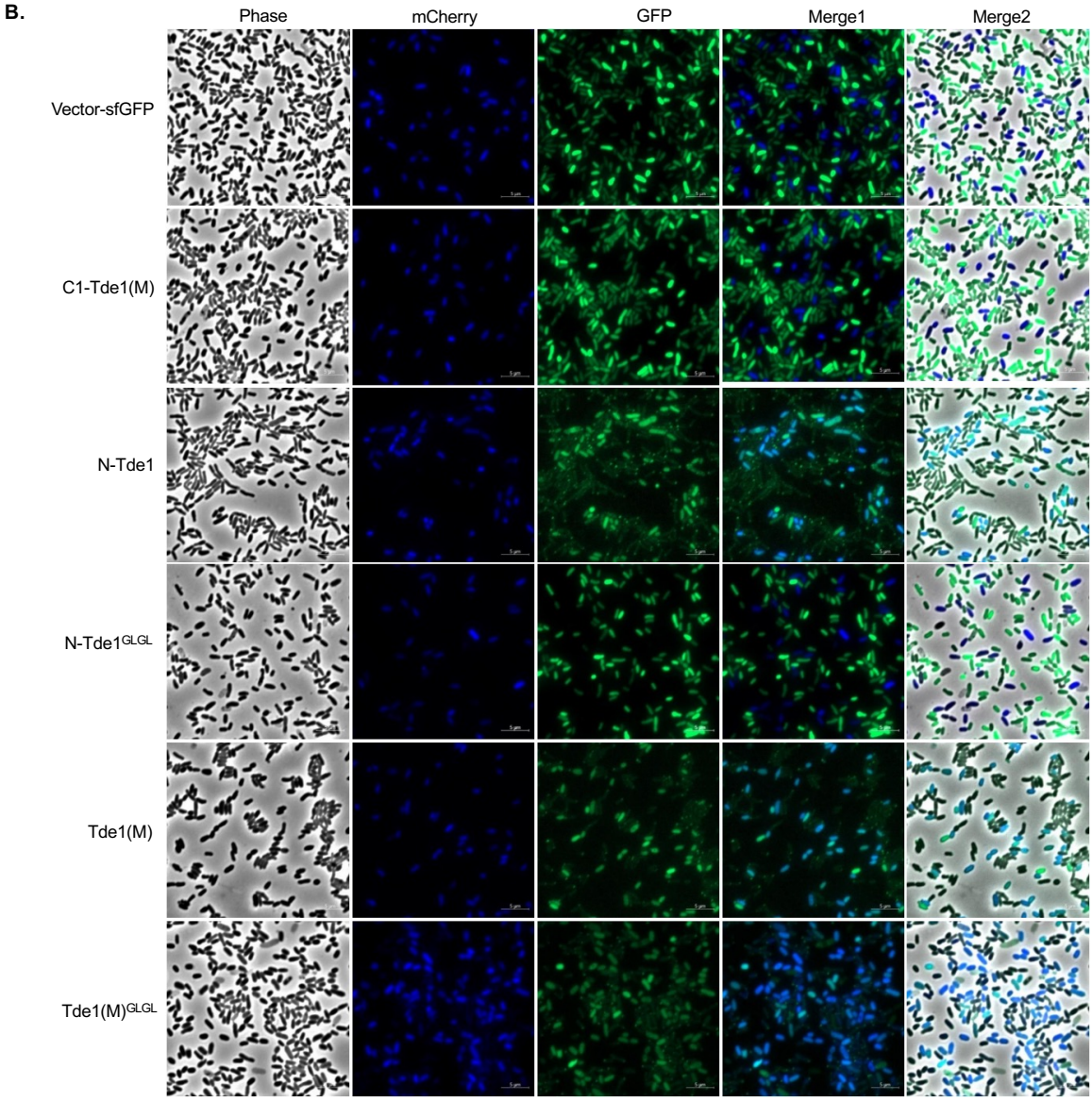

Figure 4. The roles of N-Tde1 and $G^{39}xxxG^{43}$ glycine zipper motif for secretion and translocation. (A) Secretion assay for Tde1 variants fused with sfGFP. Western blot for the cellular and extracellular fractions of *A. tumefaciens* C58 Δ*tdei* and Δ*tdei1*Δ*tssK* expressing the Tde1 variants fused with sfGFP were detected by anti-GFP antibody. Representative western blot results of three independent experiments were shown with antibody against GFP, Hcp, or EF-Tu serving as a loading and non-secreted protein control. Hcp secretion served as a positive control for active T6SS secretion. Protein markers are indicated in kDa. (B) Fluorescence microscopy for Tde1 translocation. *A. tumefaciens* C58 Δ*tdei* expressing Tde1 variants fused with sfGFP (in green) and *E. coli* DH10B carrying mCherry (false coloured in blue) were co-cultured for 20 hrs. A cyan fluorescence with merged blue and green signals represented the translocation of Tde1 variants from *A. tumefaciens* to *E. coli*.

Figure 5

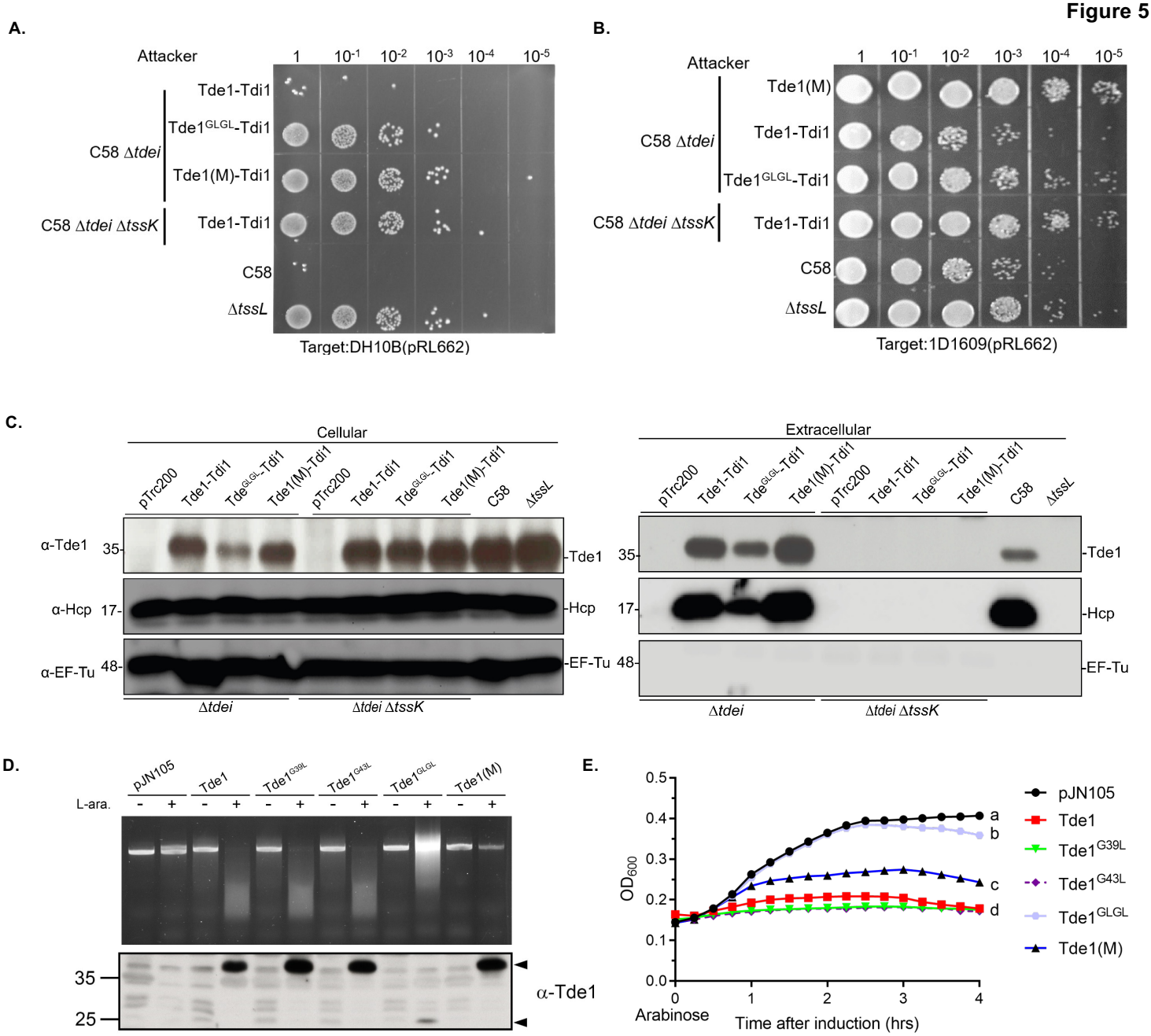

Figure 5. G[39]xxxG[43] glycine zipper motif of Tde1 is required for DNase-mediated killing of target cells during interbacterial competition. (A) Inter-species Interbacterial competition. *A. tumefaciens* C58 Δ*tdei* and Δ*tdei1*Δ*tssK* expressing the Tde1 variants were co-incubated with *E. coli* (DH10B) cells on AK medium followed by selecting target cell survival with serial dilution on a gentamycin containing LB agar at 37°C. (B) Intra-species Interbacterial competition between *A. tumefaciens* C58 *(*Δ*tdei)* and Δ*tdei1*Δ*tssK* expressing the Tde1 variants and *A. tumefaciens* 1D1609 target cell. The competition was done as in (B) except 1D1609 was recovered at 28°C. (C) Secretion assay for Tde1 and its variants co-expressed with its immunity protein Tdi1. The toxin immunity pairs Tde1-Tdi1, Tde1^{GLGL}-Tdi1, and Tde1(M)-Tdi1 were expressed in *A. tumefaciens* C58 Δ*tdei* and Δ*tdei*Δ*tssK.* (D) *In vivo* plasmid DNA degradation assay. *E. coli* BW25113 carrying pJN105 empty vector or the derivatives expressing different variants of Tde1 were supplemented with 0.5% glucose ("-") or 0.2% L-arabinose ("+") for 3 hrs to either repress or induce Tde1 production. The plasmids were then extracted to observe the DNA degradation and bottom panel showed western blots of specific Tde1 protein bands indicated by arrows. (E) Growth inhibition assay of Tde1 and its variants. *E. coli* BW25113 cells were induced by adding 0.2% L-arabinose for Tde1 production. The OD_{600} values were measured every 15 minutes. The OD_{600} values of the 4 h post L-arabinose induction were analysed for statistical analysis. Graphs show mean ± SD of three biological repeats. The significant differences were shown by the different letters (p value <0.01). All data were shown with representative results of three independent experiments. Western blots were detected with specific antibody against Tde1, Hcp, or EF-Tu serving as a loading and non-secreted protein control. Protein markers are indicated in kDa.

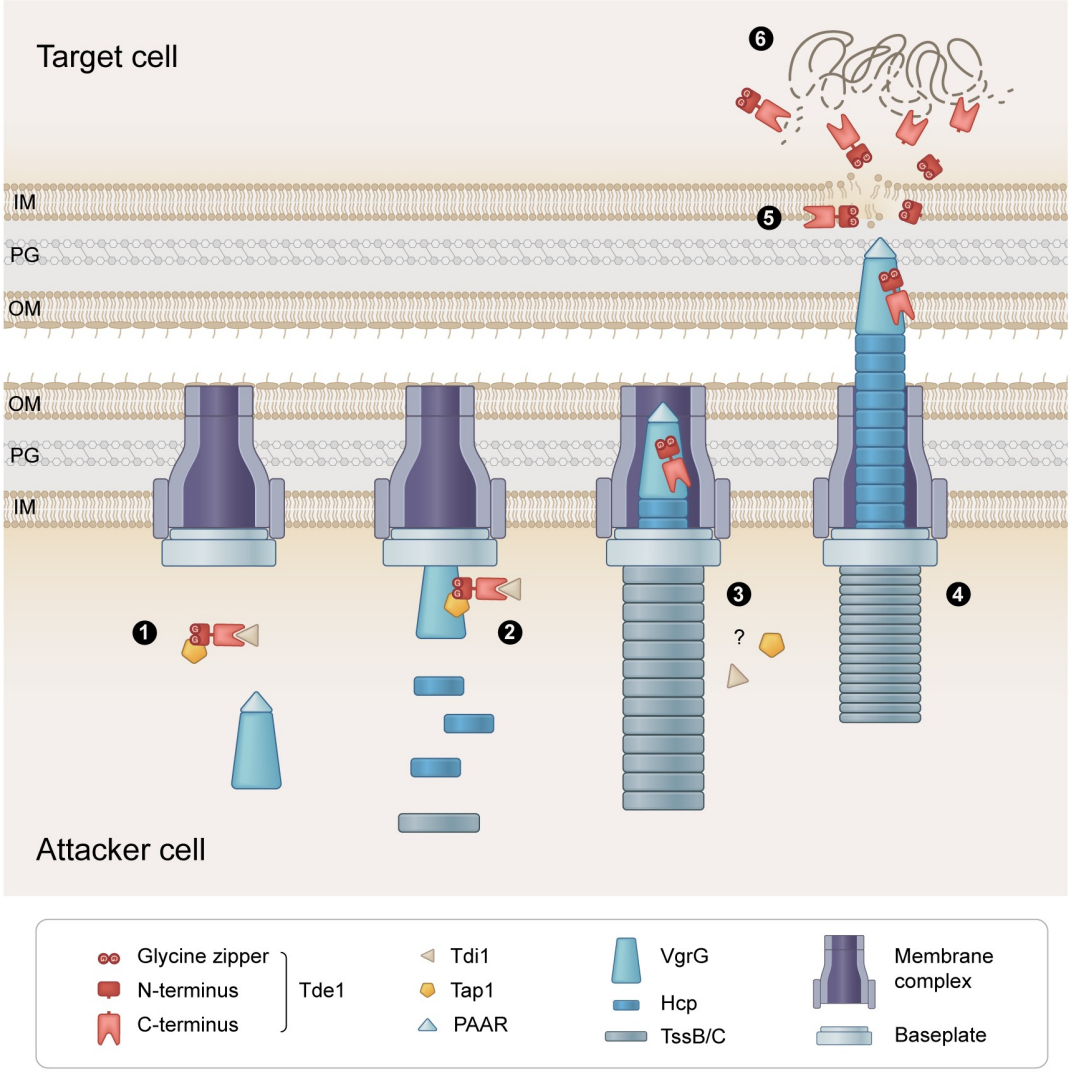

Figure 6. Proposed model of the loading, firing, and translocation of Tde1. The Tde1 translocation is proposed through six steps. Step 1: Tde1 forms a complex with Tdi1 and Tap1 in the attacker cell. Step 2: Tap1-Tde1-Tdi1 complex binds to the VgrG and the Hcp-VgrG-PAAR puncturing device carrying Tde1 effector complex is loaded onto membrane-associated baseplate. Step 3: Hcp tube and TssB/C sheath polymerize on the Tde1-loaded VgrG/baseplate while Tdi1 and Tap1 fall off with unknown mechanisms before or upon firing. Step 4: TssBC sheath contracts and ejects Tde1 into the target cell periplasm or cytoplasm. Step 5: The glycine zipper(s) on the N-terminus of Tde1 permeabilize the target cell membrane. Step 6: Intact or truncated Tde1 proteins attack DNA for degradation in the target cell.

Figure S1

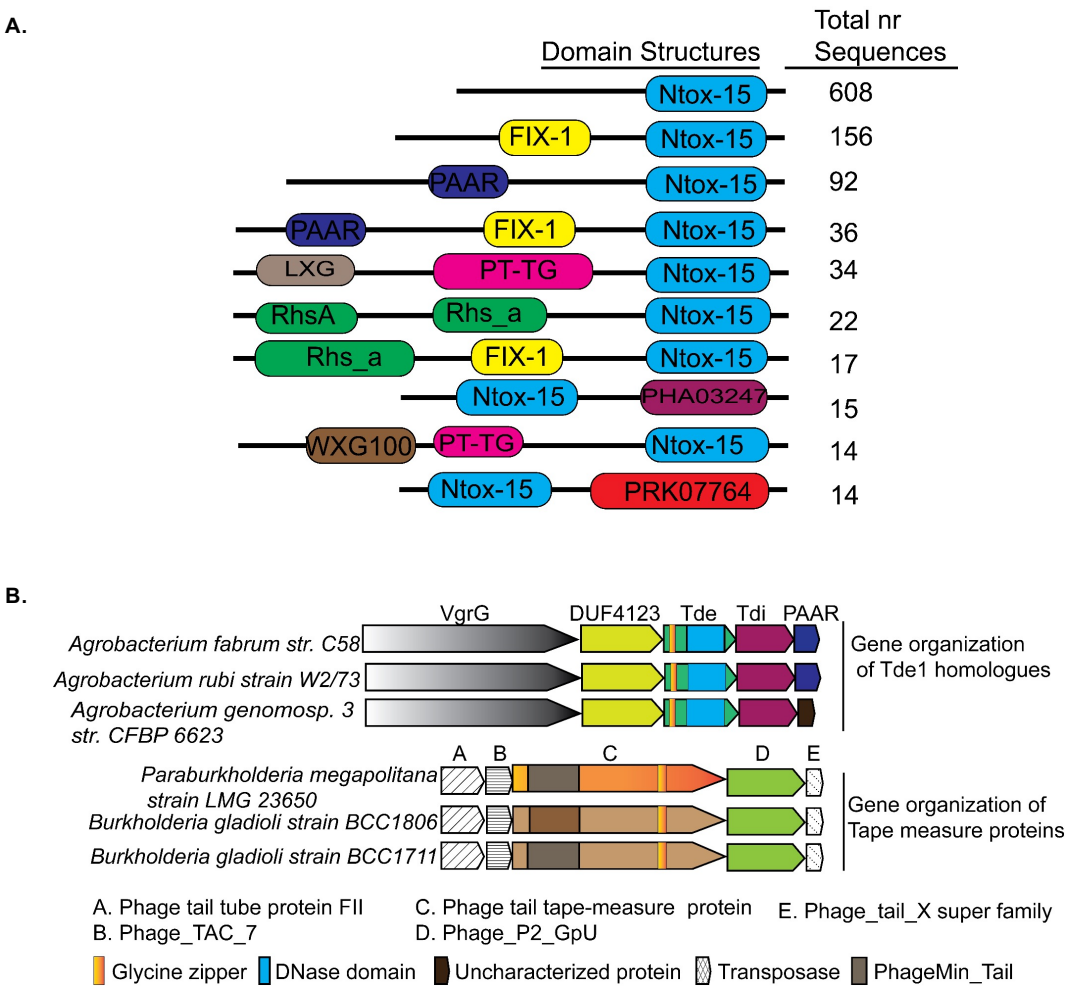

Figure S1. Domain architecture and genetic organizations of Tde homologues. (A) Domain organization of the Ntox15-containing proteins. Top 10 classes of the Ntox15-containing proteins are shown with the identifiable domains (not to scale). The number of proteins in each class were indicated on the left based on the information on June 29, 2022. The *A. tumefaciens* Tde1 belonged to the first class where the N-terminal region lacks an identifiable domain. (B) Genetic organizations of genes encoding Tde1 orthologues and Tape Measure Proteins (TMPs) with sequence similarity to N-terminus of Tde1. The proteins encoded from the upstream and downstream of *tde1* and *tmp* genes are shown with their identified domain organizations.

Figure S2

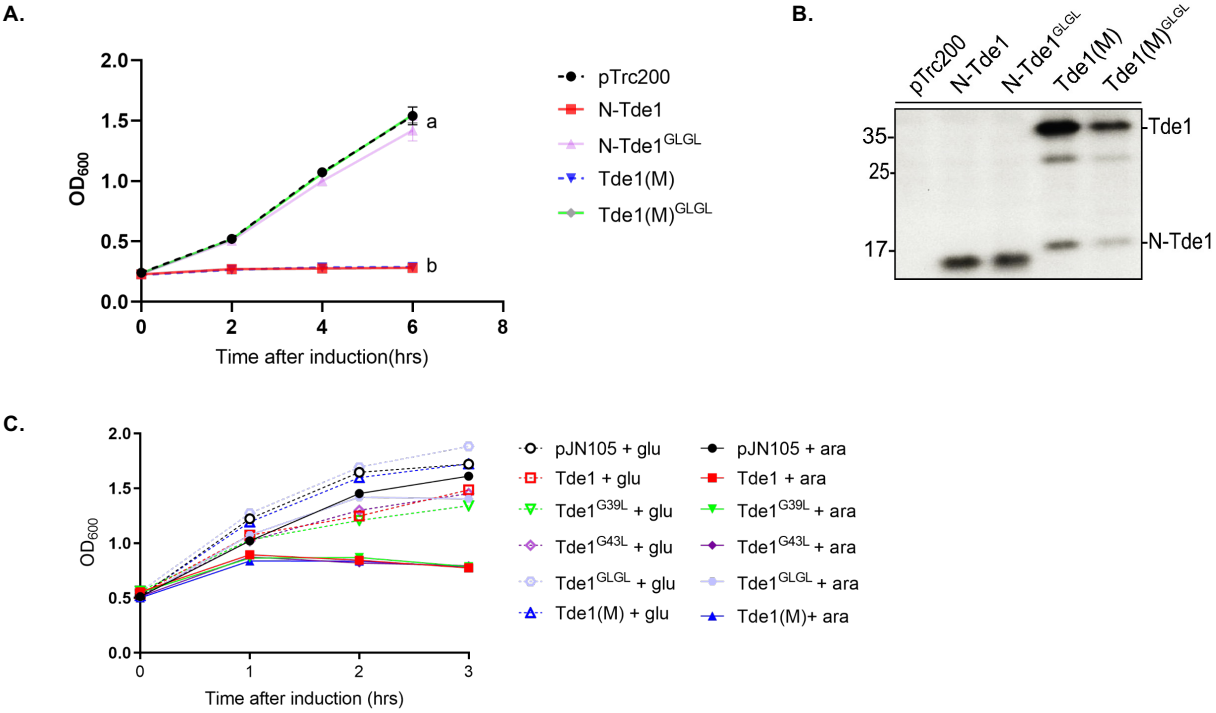

Figure S2. Growth inhibition assays in *A. tumefaciens* and *E. coli*. Growth curve (A) and western blot analyses (B) of *A. tumefaciens* C58 Δ*tde1* carrying pTrc200 or its derivatives expressing HA-tagged Tde1 variants. The growth curve was detected every 2 hrs in 523 medium supplemented with 1 mM IPTG. Graphs show mean ± SD of three independent experiments. The significant differences were shown by the different letters (p value <0.01). The proteins collected at end point (6 hr) were analysed for western blotting with antibody against HA. Representative results of three independent experiments were shown. Protein markers are indicated in kDa. (C) The growth curve analysis of *E. coli* cells used for *in vivo* plasmid DNA degradation assay. The turbidity of *E. coli* BW25113 expressing Tde1 and its variants carried out for the *in vivo* plasmid DNA degradation assay were measured. The *E. coli* cells were supplemented with 0.5% glucose (glu) or 0.2% L-arabinose (ara) for the repression or induction of Tde1 and its variants. The OD_{600} values were measured by DEN-600 photometer (Biosan, Latvia) every hr.

Figure S3

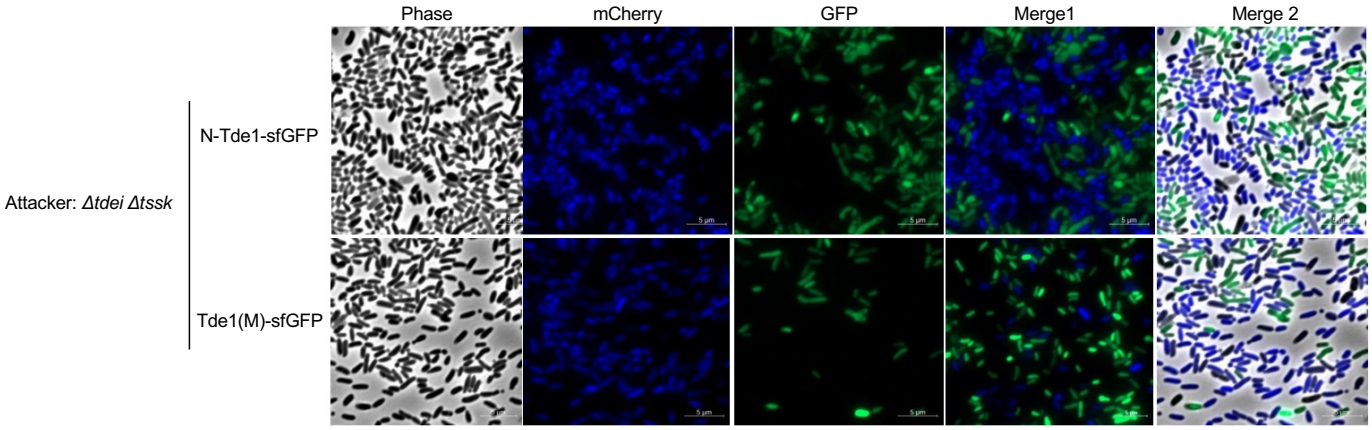

Figure S3. Fluorescence microscopy for negative controls of translocation assay.
A. tumefaciens C58 Δ*tdei*Δ*tssK* expressing N-Tde1-sfGFP or Tde1(M)-sfGFP (in green) and *E. coli* DH10B carrying mCherry (false coloured in blue) were co-cultured for 20 hrs. No cyan fluorescence with merged blue and green signals could be detected when attacker cells are T6SS-inactive, which served as negative controls for the translocation assay.

Figure S4

A.

Positions on Tde1	Alignment Coverage	3D Model	Confidence	% i.d.	Template Information
10-62	Alignment		77.3	26	**PDB header:**antimicrobial protein **Chain:** A: **PDB Molecule:**pyocin s5; **PDBTitle:** structural mechanism of pyocin s5 import into pseudomonas aeruginosa **PDB Entry:** PDBe RCSB PDBj ✓ View investigator results
14-58	Alignment		69.5	18	**PDB header:**transmembrane protein **Chain:** A: **PDB Molecule:**colicin ia; **PDBTitle:** colicin ia **PDB Entry:** PDBe RCSB PDBj Run Investigator
7-62	Alignment		33.0	25	**Fold:** Toxins' membrane translocation domains **Superfamily:** Colicin **Family:** Colicin **PDB entry:** PDBe RCSB PDBj Run Investigator
19-51	Alignment		27.6	50	**PDB header:**viral protein/inhibitor **Chain:** C: **PDB Molecule:**envelope glycoprotein b; **PDBTitle:** hcmv prefusion gb in complex with fusion inhibitor way-174865 **PDB Entry:** PDBe RCSB PDBj Run Investigator
4-62	Alignment		27.4	27	**PDB header:**immune system **Chain:** X: **PDB Molecule:**colicin s4; **PDBTitle:** structure and function of colicin s4, a colicin with a duplicated2 receptor binding domain **PDB Entry:** PDBe RCSB PDBj Run Investigator

B.

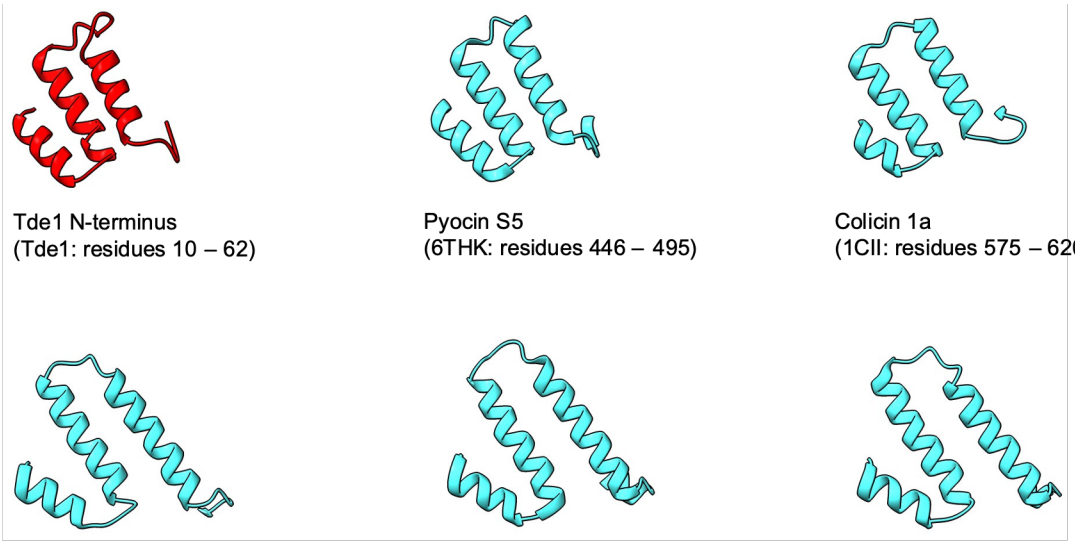

C.

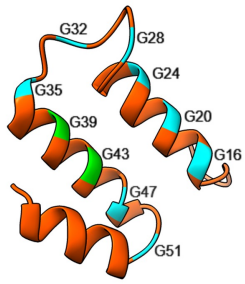

D.

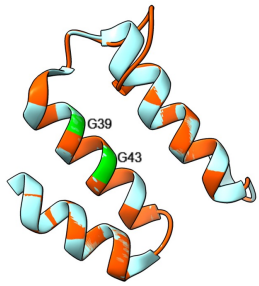

Figure S4. Structural prediction of the Tde1 N-terminus with similarity to pyocin S5 and colicins. (A) Predicted results of N-terminal Tde1 (1-97) as a query. (B) N-terminal Tde1 with structural similarity to pore-forming domain of the pyocin S5, colicines and other membrane perturbing proteins based on Phyre2 prediction. (C) Cartoon model of the Tde1 (residue 10 – 62) by using on the basis of the crystal structure of Pyocin S5 (PDB 6THK) with 77.3% of identity. Glycine residues of Tde1 were indicated. (D) Superimposition of N-Tde1 and pore-forming domain of pyocin S5. Tde1 N-terminus is in red and partially pore-forming domain of pyocin S5 is in teal, G^{39} and G^{43} in the putative glycine zipper motif are highlighted in green. All data were analyzed by Phyre2 server.